NITROUS OXIDE PRODUCTION IN THE GULF OF MEXICO HYPOXIC ZONE

A Thesis

by

LINDSEY A. VISSER

Submitted to the Office of Graduate Studies of
Texas A&M University
in partial fulfillment of the requirements for the degree of

MASTER OF SCIENCE

August 2009

Major Subject: Oceanography

NITROUS OXIDE PRODUCTION IN THE GULF OF MEXICO HYPOXIC ZONE

A Thesis

by

LINDSEY A. VISSER

Submitted to the Office of Graduate Studies of
Texas A&M University
in partial fulfillment of the requirements for the degree of

MASTER OF SCIENCE

Approved by:

Chair of Committee,	Daniel C. O. Thornton
Committee Members,	Thomas S. Bianchi
	Gunnar Schade
Head of Department,	Piers Chapman

August 2009

Major Subject: Oceanography

ABSTRACT

Nitrous Oxide Production in the Gulf of Mexico Hypoxic Zone.

(August 2009)

Lindsey A. Visser, B.S., Texas A&M University

Chair of Advisory Committee: Dr. Daniel C. O. Thornton

The Gulf of Mexico hypoxic zone is created by strong persistent water stratification and nutrient loading from the Mississippi River which fuels primary production and bacterial decomposition. The Texas-Louisiana shelf becomes seasonally oxygen depleted and hypoxia ($O_2 \leq 1.4$ ml l^{-1}) occurs. Low oxygen environments are conducive for the microbial production of nitrous oxide (N_2O), a powerful greenhouse gas found in the atmosphere in trace amounts (319 ppbv). Highly productive coastal areas contribute 61% of the total oceanic N_2O production and currently global sources exceed sinks.

This study is the first characterization of N_2O produced in the Gulf of Mexico hypoxic zone. Because of enhanced microbial activity and oxygen deficiency, it is hypothesized that the Gulf of Mexico hypoxic zone is a source of N_2O to the atmosphere. Seasonal measurements of N_2O were made during three research cruises in the Northern Gulf of Mexico (Sept. 2007, April 2008, and July 2008). Water column N_2O profiles were constructed from stations sampled over time, and bottom and surface samples were collected from several sites in the

hypoxic zone. These measurements were used to calculate atmospheric flux of N_2O.

The Gulf of Mexico hypoxic zone was a source of N_2O to the atmosphere, and N_2O production was highest during times of seasonal hypoxia. N_2O was positively correlated with temperature and salinity, and negatively correlated with oxygen concentration. Atmospheric fluxes ranged from -11.27 to 153.22 μmol m^{-2} d^{-1}. High accumulations of N_2O in the water column (up to 2878 % saturated) were associated with remineralization of organic matter at the base of the pycnocline and oxycline. Seasonal hypoxia created a source of N_2O to the atmosphere (up to 2.66 x 10^{-3} Tg N_2O for the month of September 2007), but there was a slight sink during April 2008 when hypoxia did not occur. Large fluxes of N_2O during the 3 to 5 month hypoxic period may not be counterbalanced by a 7 to 9 month sink period indicating the Gulf of Mexico hypoxic zone may be a net source of N_2O to the atmosphere.

DEDICATION

I would like to dedicate this research to my parents, Loren and Pamela Visser, for their love and support throughout my academic career. They have always encouraged my curiosity and instilled in me the confidence to pursue my goals.

ACKNOWLEDGEMENTS

I would like to especially like to thank my committee chair, Dr. Daniel Thornton, for his continuous dedication and support, and also my committee members, Dr. Thomas Bianchi and Dr. Gunnar Schade, for their guidance throughout the course of this research.

Thanks also go to Dr. Steven DiMarco for providing the opportunity to participate in Mechanisms Controlling Hypoxia cruises, to Dr. Matt Howard for providing the cruise data, and Dr. Heath Mills and Dr. Shari Yvon-Lewis for all of their assistance.

I would also like to thank Federico Alvarez, Brandi Kiel Reese, Julia O'Hern, Ruth Mullins, and Clifton Nunnally for assistance with sample collection, Kelly Cole, Jason Moore, and Christina Wiederwohl for assistance with graphing and statistics, Richard Smith and Stella Woodard for their revisions, and the crew of the LUMCON R/V Pelican for all their hard work.

NOMENCLATURE

CTD	Conductivity Temperature Depth
DIN	Dissolved Inorganic Nitrogen
DNRA	Dissimilatory Nitrate Reduction to Ammonium
DO	Dissolved Oxygen
EPA	Environmental Protection Agency
IPCC	Intergovernmental Panel on Climate Change
LUMCON	Louisiana University Marine Consortium
M10	Mechanisms Controlling Hypoxia Cruise 10 (6-9 September 2007)
M11	Mechanisms Controlling Hypoxia Cruise 11 (16-19 April 2008)
M12	Mechanisms Controlling Hypoxia Cruise 12 (17-20 July 2008)
N_2O	Nitrous Oxide

TABLE OF CONTENTS

Page

LIST OF FIGURES

Page

LIST OF TABLES

1. INTRODUCTION

1.1 Background

Seasonal hypoxia in the Northern Gulf of Mexico has become an environmental concern in recent decades. Hypoxia is the occurrence of reduced dissolved oxygen (DO) concentrations in the range of 3.0 to 0.2 ml l^{-1}, with a general consensus defining it to be ≤ 1.4 ml l^{-1} (2 mg l^{-1}). Coastal hypoxia is often created by river outflow, which causes strong persistent water stratification and delivers nutrients to the surface waters, which fuels high rates of primary production (CENR 2000). This marine organic material fluxes to the lower water column and seabed in the form of senescent phytoplankton and zooplankton aggregates or fecal pellets. As a result of bacterial decomposition of this organic matter, oxygen is consumed faster than it is re-supplied from the overlying the water column. This process paired with strong water stratification develops hypoxia in the bottom waters (Rabalais et al. 2007). Massive inputs of fresh water, seasonal variance in stratification strength, weak tidal action, and high average water temperature influence hypoxia in the Northern Gulf of Mexico (Hetland & DiMarco 2008). The average size of the hypoxic zone as well as the duration of each event has increased over the past 50 years in relation to enhanced nutrient loading (Osterman et al. 2005, EPA 2007). Nutrient input is correlated with river outflow, indicating hypoxia is dependent upon both nutrient induced eutrophication and water stratification.

This thesis follows the style of Marine Ecology Progress Series.

Hypoxia in the Northern Gulf of Mexico extends 125 km offshore to 60 m depth. The average mid-summer areal extent is 16,500 km^2 (since 2001) beginning at the mouth of the Mississippi River and extending as far west as the coastal waters of Texas Preliminary oxygen data indicates that hypoxia reached 20,720 km^2 in 2008, making it the second largest event on record (LUMCON 28 July 2008). The major source of freshwater, nitrogen, and phosphorus to the hypoxic zone in the Northern Gulf of Mexico is the Mississippi River. It has an annual average discharge of 580 km^3, and has the largest watershed in North America (Rabalais et al. 2007), draining approximately 48% of the continental United States. Its two major distributaries, the Birdfoot delta and the Atchafalaya River delta, along with many rivers along Louisiana and Texas Coast including the Trinity River, influence the hypoxic zone. The Mississippi and Atchafalya rivers account for 96% of the annual freshwater discharge, 98.5% of the annual nitrogen load, and 98% of the annual phosphorus load into the zone most likely to influence hypoxia (Rabalais et al. 2007).

Ecosystem responses to hypoxia include diminished biodiversity and altered community structure (Rabalais et al. 2001). Long exposure to hypoxia creates low annual secondary production and loss of benthic fauna (Diaz & Rosenberg 2008). Without benthic fauna, denitrification is disrupted from the lack of bioturbation, and microbial decomposition dominates (Diaz and Rosenberg 2008). Oxygen thresholds vary across taxa, with crustaceans being the most oxygen sensitive organisms, and molluscs, cnidarians, and priapulids the most tolerant (Vaquer-Sunyer & Duarte 2008). Mechanisms benthic organisms use to cope with hypoxia include leaving their burrows or tubes, reducing burial depth, or shifting to anaerobic metabolism for a period of hours to

days which is seen in polychaetes, oligochaetes, echinoderms, and the mud shrimp *Calocaris mancandreae* (Vaquer-Sunyer & Duarte 2008 and sources therein).

1.2 Nitrous Oxide

Nitrous oxide is a greenhouse gas found in the troposphere at trace concentrations of 319 ppbv averaged globally (IPCC 2007). Global N_2O concentrations have increased since pre-industrial times from 270 ppb to 319 ± 0.12 ppb in 2005, and since 1998 it has increased by 5 ppb (IPCC 2007). One molecule of N_2O has 200 to 300 times more warming potential than one molecule of carbon dioxide (Table 1). It has the fourth highest radiative forcing (RF) of all the long-lived greenhouse gases (IPCC 2007) (Table 1). N_2O does not react with hydroxyl radicals in the troposphere; rather, it lacks any vertical gradient until it reaches the stratosphere where it has a lifetime of 114 years (Montzka et al 2003). In the stratosphere, UV light photochemically destroys N_2O to form nitric oxide (NO). Nitric oxide destroys the UV-protective ozone layer in the stratosphere (Bange 2000). Ozone loss increases the amount of UV that photolyzes N_2O, creating a feedback that perturbs the lifetime of N_2O (IPCC 2001). For every 10% increase in N_2O, its atmospheric lifetime decreases by 0.5% (IPCC 2001).

Total N_2O surface emissions when combined with stratospheric loses are 16 TgN yr^{-1}, and the Northern hemisphere contributes 60% of this. Nitrous oxide concentrations have risen by 9 %, or 27 ppbv since pre-industrial times, and global anthropogenic emissions are estimated at 7 ± 1 Tg yr^{-1} (Khalil & Rasmussen 1992, Khalil et al. 2002). The annual growth rate of N_2O in the troposphere is about 0.25 to 0.31 % yr^{-1} (Weiss

1981, Khalil & Rasmussen 1992), indicating global sources exceed sinks (Bouwman et al. 1995).

Table 1. The contribution of various gases, relative to CO_2, to the greenhouse effect. Calculations are based on emitted amounts, and consideration has been given to the gases' decay in the atmosphere. (Modified from Rhode 1990).

Species	Relative contribution: Mass basis (kg^{-1})	Relative contribution: Mole basis (mol^{-1})
CO_2	1	1
O_3 (in troposphere)	3	4
CH_4 (direct effects)	15	5
CH_4 (including indirect effects)	30	10
N_2O	300	300
CFC-11	4,000	11,000
CFC-12	8,000	20,000

Natural sources of N_2O are soils and the ocean, whereas anthropogenic sources are use of nitrogen-based fertilizers enhancing the soil source, cattle feedlots, wastewater treatment, automobiles, and industrial manufacturing, such as Nylon production (Khalil et al. 2002). The ocean contributes 0.3 to 6.6 TgN yr^{-1}, which is 30 % of all atmospheric N_2O. Coastal sources of N_2O are estimated at 0.2 TgN yr^{-1} (Nevison et al. 2004). 61 % of oceanic N_2O production comes from highly productive coastal areas such as upwelling, continental shelves, rivers, and estuaries (Bange et al. 1996, Nevison et al. 2004, Kroeze et al. 2005). Nitrous oxide saturation has only been measured in a minor part of the world's oceans, the measurements of seasonal differences are insufficient, and global estimates may have up to 50 % uncertainty (Bouwman et al. 1995). The major driver for industrial era N_2O production is considered to be enhanced microbial production (IPCC 2007). The atmosphere is generally in equilibrium with surface N_2O concentrations in the ocean, but there is a subsurface accumulation associated with the oxygen minimum zone (Bange et al. 2001). In many productive estuaries, the water

column is supersaturated with N_2O and it is a source to the atmosphere (Dong et al. 2002, Dong et al. 2006). The Northern Gulf of Mexico hypoxic zone is also highly productive and subject to freshwater influx, which indicates the shelf water may display both estuarine characteristics, and processes similar to that of oceanic oxygen minimum zones. Naqvi et al. (2000) found that hypoxic coastal waters off of the western Indian shelf lead to an increase in N_2O production and emission. The highest N_2O concentrations occurred in suboxic waters and exceeded 533 nM, the surface waters had a maximum of 436 nM and were 8,250% saturated. For the study area of 180,000 km^2 they estimated N_2O efflux to be 0.06-0.39 Tg N_2O over a 6 month period, similar to that of the entire Arabian Sea.

Until now, no direct measurements of N_2O flux from the sediments or water column have been taken in the Gulf of Mexico hypoxic zone. The production of N_2O in this region must be taken into account when considering regional and global geographic distribution budgets of N_2O emissions.

The marine environment plays a major role in the cycling of N_2O, which is driven by the activities of microorganisms (Bange 2000). Two main processes that produce N_2O in the ocean are nitrification and denitrification (Fig 1). Nitrification is the microbial transformation of ammonium into nitrate releasing N_2O as a by-product, and it is the main source for oceanic N_2O (Butler et al. 1989). This two-step process involves oxidation of ammonium to nitrite, which releases N_2O, and then further oxidation of nitrite to nitrate (Bonin et al. 2002). Nitrification may be the predominant source of N_2O in oxic conditions, but denitrification appears to be the dominant source in hypoxic conditions (Punshon & Moore 2004).

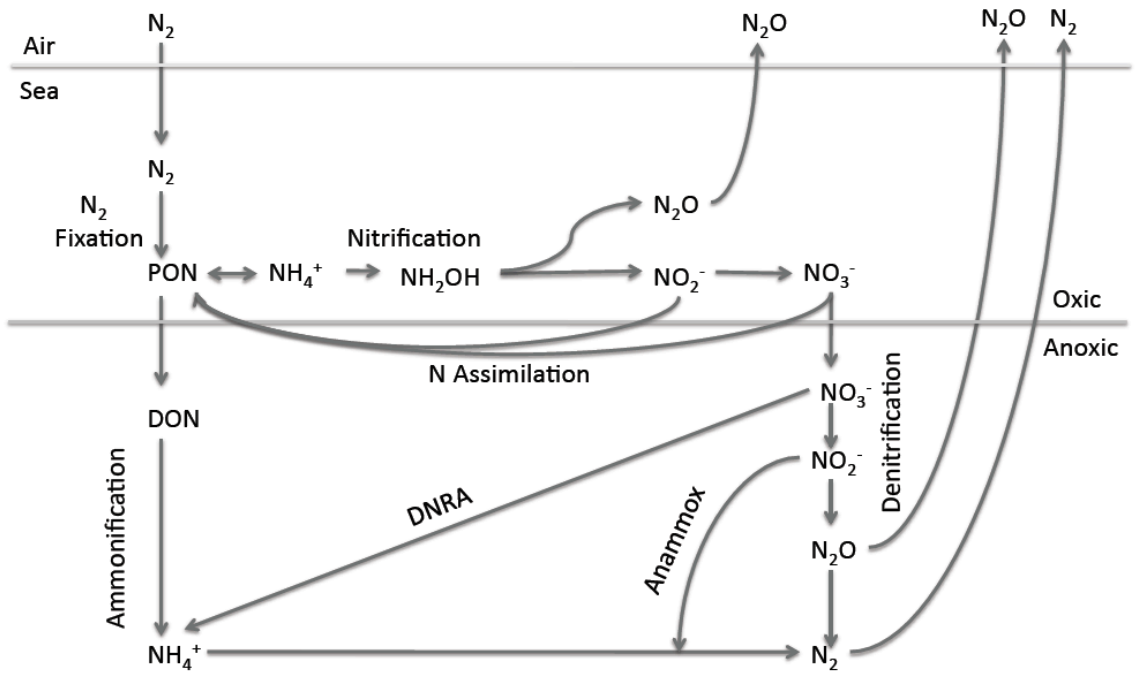

Figure 1. The marine nitrogen cycle showing the major pathways of N_2O production (Modified from Arrigo 2005).

Denitrification involves anaerobic microbial respiration reducing nitrate or nitrite into N_2O or nitrogen gas (N_2), and it is a major sink for fixed nitrogen in the Gulf of Mexico hypoxic zone (Childs et al. 2002). Denitrification is carried out through four independent respiratory processes, often by an assemblage of different bacteria (Zumft 1997). Nitrous oxide may be released as a by-product or end product of this transformation (Bange 2000). Most denitrifiers are facultatively aerobic, and low oxygen environments cause an accumulation of N_2O (Jorgensen et al. 1984, Zumft 1997). The hypoxic zone has large fluxes of organic matter and low DO concentrations signifying denitrification rates may be quite high (Gardner et al. 1993). But reported potential denitrification rates in this area are wide-ranging (39.8 and 108.1 μmol m^{-2} h^{-1}), depending upon salinity and temperature (Childs et al. 2002). Childs et al. (2002) showed that denitrification rates in the Gulf of Mexico hypoxic zone were highest when oxygen concentrations were between 1 and 3 mg l^{-1}. Below 1 mg l^{-1}, denitrification rates

were unexpectedly low when compared to other systems possibly due to nitrogen limitation and anaerobic microbial competition favoring dissimilatory nitrate reduction to ammonium (DNRA), which is reduction of nitrate or nitrite to ammonium (Childs et al. 2002). Another possibility for low denitrification rates is that nitrification is inhibited under low oxygen conditions, so nitrate is not available for denitrification (Sloth et al. 1995).

DNRA is advantageous with a limited concentration of electron acceptors in the system because it accommodates more electrons per molecule of nitrate (8) compared with denitrification (5). Senga et al. (2006) found N_2O accumulation in the sediments of two lakes to be derived not only from denitrification, but also from DNRA in the presence of H_2S. Sulfate reduction is a major anaerobic metabolic respiratory pathway in sediments lacking oxygen (Rowe 2001). Sediments in the hypoxic zone may then be a source of N_2O via DNRA because of the presence of H_2S and enhanced microbial activity from organic matter accumulation.

Increased anthropogenic N inputs are known to increase microbial processes involved in nitrogen cycling, which results in increased N_2O production (Seitzinger & Kroeze 1998). Coastal systems are generally nitrogen limited due to the N sink from denitrification. In areas of oxygen depletion, nitrification, denitrification, or a coupling of the two produce N_2O (Bange et al. 2001, De Bie et al. 2002). The transition zones between aerobic and anaerobic conditions are conducive for N_2O production. Nitrogen loading that enters the hypoxic zone from the Mississippi River coupled with low oxygen levels indicates that the hypoxic zone may be a source of N_2O accumulation in the water column, and a subsequent source to the atmosphere.

1.3 Hypothesis

The central hypothesis for this research is that *coastal hypoxic zones are significant sites for N_2O production due to the low oxygen and high inorganic nitrogen concentrations in the water column.*

The objectives of this proposed research are:

- To determine whether there is a net flux of N_2O from the water column to the atmosphere. From this, predictions of air-sea flux rates of N_2O in the Gulf of Mexico hypoxic zone can be made.
- To observe seasonal changes in N_2O production associated with seasonal hypoxia.
- To determine how N_2O vertical distribution varies over time with changes in oxygen conditions, salinity, temperature, and nutrient (NO_3^-, NO_2^-, NH_4^+) concentrations.
- To examine the role of sediments in the hypoxic zone as a possible source of N_2O to the overlying water column and atmosphere.

With these research objectives, further hypothesis can be formed:

The Gulf of Mexico hypoxic zone is a source of N_2O to the atmosphere.

The rationale for this hypothesis is that N loading fuels oxidation of organic matter at the seafloor, and this coupled with persistent water stratification creates seasonal hypoxia. Low oxygen conditions are conducive for N_2O production via denitrification, nitrification, or DNRA.

There will be distinct seasonal changes in N_2O production associated with seasonal hypoxia. N_2O production will be highest in the summer when hypoxia is the strongest, and low in the spring before its onset.

Water column N_2O concentrations are higher at night than during the day. This is because water column oxygen concentrations are lower during the night from the consumption of oxygen through respiration, and the lack of photosynthetic activity.

Sediment in the hypoxic zone is a source of N_2O to the overlying water column. This is due to the hypoxic or anoxic nature of the sediments, which creates biological assemblages of microorganisms capable of denitrification, nitrification, and DNRA which all produce N_2O. These environments also undergo sulfate reduction to produce H_2S, which enhances DNRA. Also, sediments themselves are rich in organic matter and have high biological activity to fuel respiration.

2. METHODS

2.1 Study Area

Research was conducted aboard the *R/V Pelican*, operated by LUMCON: Louisiana University Marine Consortium (Cocadrie, LA) during three Mechanisms Controlling Hypoxia (MCH) Cruises: M10 (6-9 September 2007), M11 (16-19 April 2008), and M12 (17-20 July 2008). Locations of N_2O sampling stations are shown for the M10 (Fig. 2), M11 (Fig. 3) and M12 (Fig. 3) cruises. These dates provided adequate coverage in order to display seasonal variations in hypoxia. The M10 and M12 are summer cruises when hypoxia is typically most extreme and water stratification high froming a strong pycnocline generated from warmer temperatures and increased river runoff from the spring melt. In the spring (M11) there is generally less hypoxia due to lower temperatures and less water stratification.

Stations were labeled by zone (denoted by a number followed by A, B, C, or D) according to Rowe and Chapman (2002). Zone A (not sampled) is located near the mouth of the Mississippi River and it is generally characterized by high sediment deposition, which decreases light availability and causes low primary production. Zone B is located between the Mississippi and Atchafalaya Rivers where high primary production occurs as a result of high nutrient input. Hypoxia further westward in zone C is physically controlled by water stratification, and productivity results from regenerated nitrogen. Zone D has recently been added due to the increase in size of the hypoxic zone and it is hypothesized that benthic respiration, rather than river-plume dependent respiration plays a key major role in maintaining hypoxia further westward.

Classification of zones is very general and these regions may shift according to environmental factors, i.e. variations in river output, seasonal changes, and storm events.

During each cruise, station 8C was sampled every 4 hours to produce a series of depth profiles over the course of 12 to 36 hours. On all cruises, sampling at station 8C began at 12am, and sampling continued every 4^{th} hour for at least 12 hours. Station 8C for M10 lasted 36 hours, M11 lasted 12 hours and M12 lasted for 24 hours but has missing data due to inclement weather. For the rest of the stations listed, bottom and surface water were collected using either a bucket on the surface, or a Niskin bottle at the bottom. Stations 7B, 8B, 9B, and 10B as well as stations 7C, 8C, 9C, and 10C represent depth transects from the 10 to 30 m isobaths. The stations were intended to be kept constant for every cruise, but they vary slightly each cruise due to changing cruise plans, inclement weather, or omission of stations from the cruise track. Where stations could not be repeated, the nearest station to the original location was sampled.

Water samples were collected with a 12 Niskin bottle (10 L each) rosette/CTD/ and a bottom-landing 4 bottle (1.5 L each) rosette/CTD/transmissometer. Water from the air-sea interface was collected using a bucket lowered over the side of the vessel. Hydrographic data was obtained using a SeaBird CTD system. Data provided by collaborators (Steven DiMarco et al.) included temperature, dissolved oxygen (DO) (Winkler titrations), conductivity, salinity, and depth. Water samples for nutrient analysis (NO_3^-, NO_2^-, NH_4^+) were 0.2 μm filtered and frozen on board for later analysis by technicians at the Geochemical and Environmental Research Group (GERG), Texas A&M University. Nutrients were analyzed according to established protocols (Armstrong et al. 1967, Bernhardt & Wilhelms. 1967, Harwood et al 1970, Kirkwood

1996) using a Technicon II AA nutrient autoanalyzer.

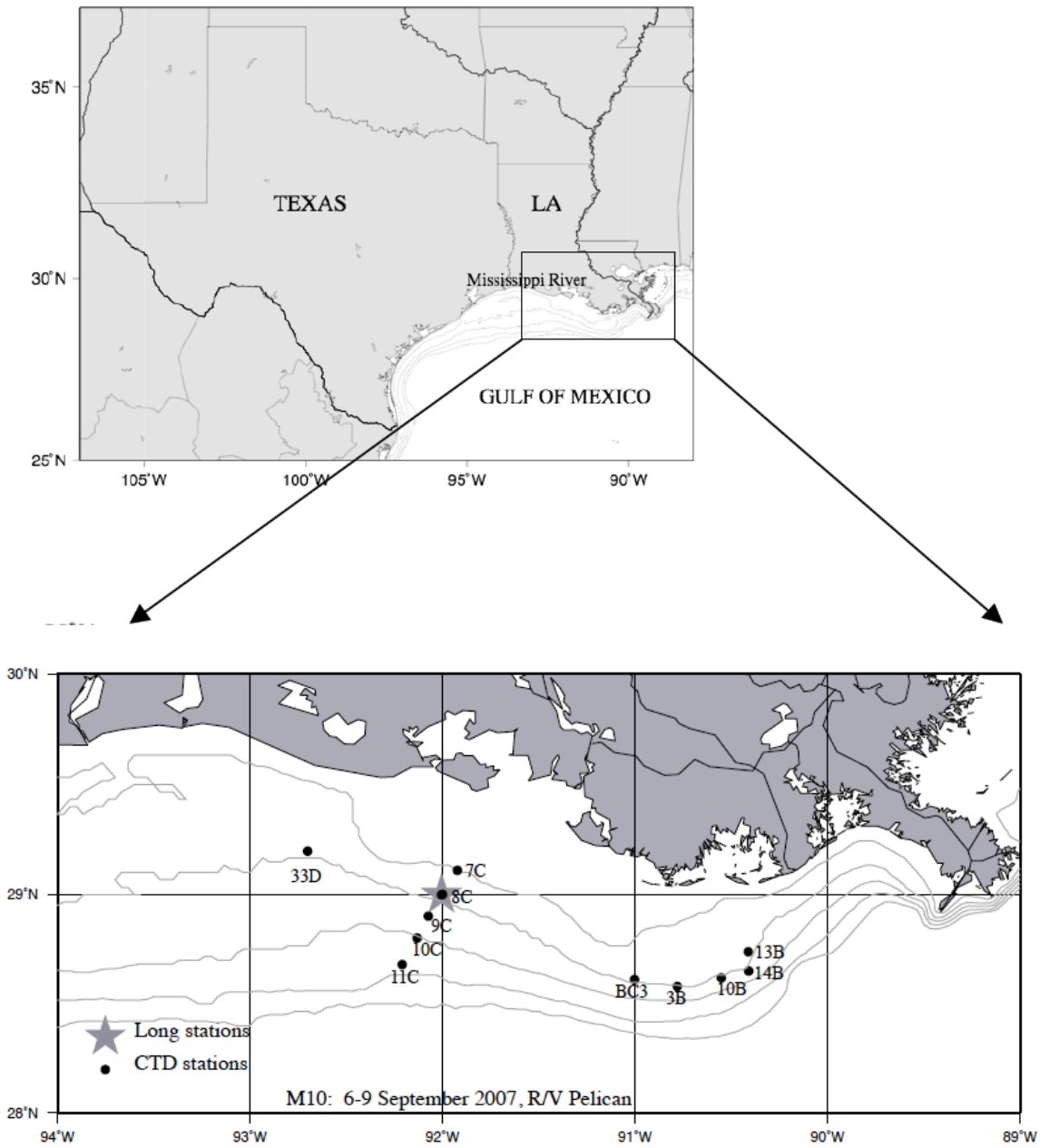

Figure 2. Map of study area showing regional scale and locations of NOAA/TAMU CTD and N_2O stations for the M10 (September 2007). Shown are the 10, 20, 30, 40, and 50 m isobaths derived from the DBDB2 bathymetry database (Modified from map produced by Steven DiMarco).

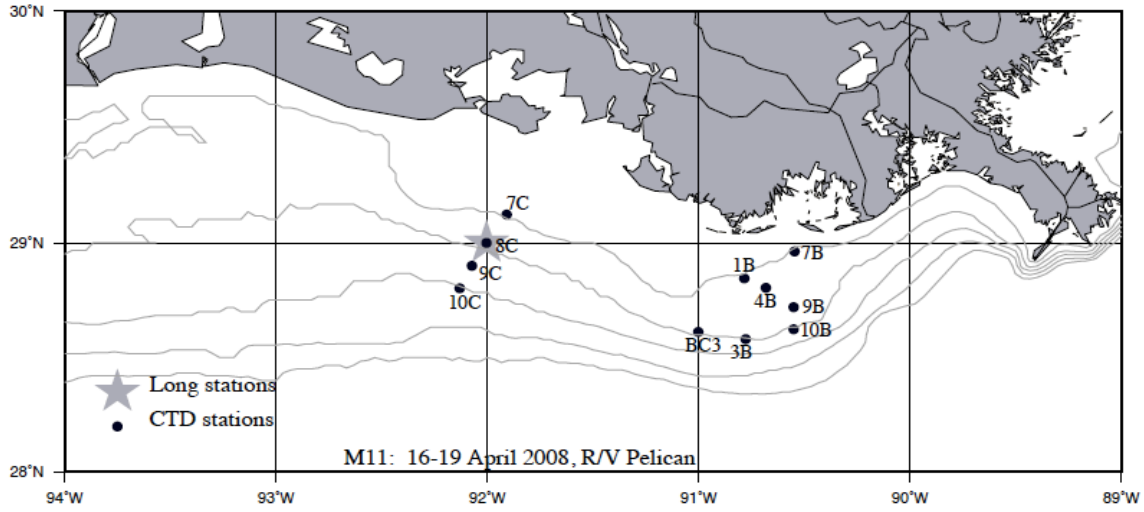

Figure 3. Locations of NOAA/TAMU CTD and N_2O stations for M11 (April 2008). Shown are the 10, 20, 30, 40, and 50 m isobaths derived from the DBDB2 bathymetry database (Modified from Steven DiMarco).

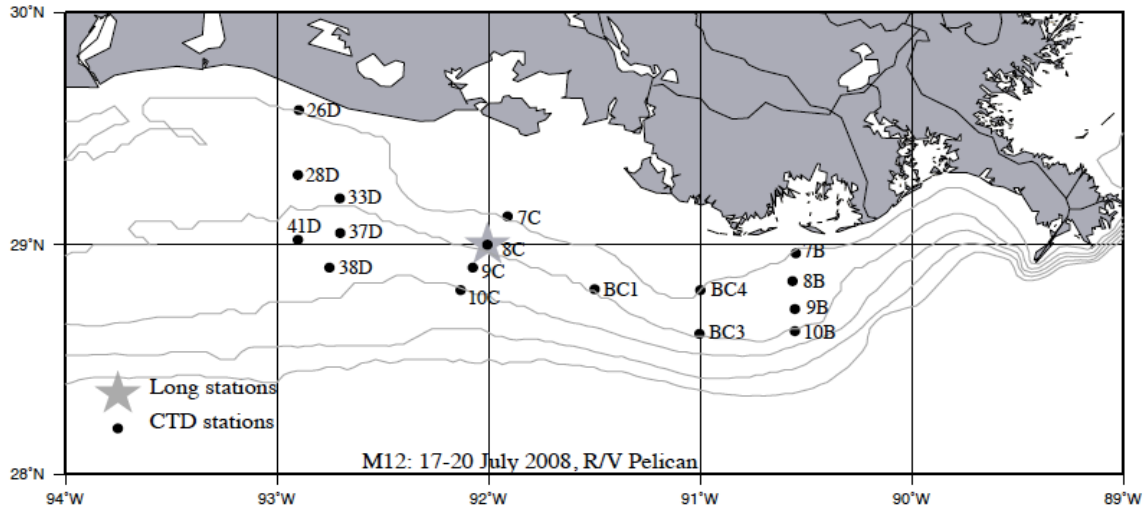

Figure 4. Locations of NOAA/TAMU CTD and N_2O stations for M12 (July 2008). Shown are the 10, 20, 30, 40, and 50 m isobaths derived from the DBDB2 bathymetry database (Modified from Steven DiMarco).

2.2 N_2O Methodology

Water samples were collected for N_2O in triplicate through Teflon tubing attached to the Niskin bottle. The water was allowed to overflow at least three volumes into a 20 ml glass headspace analysis vial (Agilent Technologies). The vials were then preserved

with a 2% formalin solution (w/v), quickly sealed, and crimped with 20 mm Teflon lined silicone seals (Agilent Technologies). Care was taken to exclude air bubbles during sampling and sealing, and samples containing air bubbles were re-collected or discarded. Surface water that was collected with a bucket was sampled immediately to avoid equilibration with the atmosphere. Vials were stored in the dark at 4 ºC and analyzed within 1 month at the Microbial Ecology and Biogeochemistry Laboratory, Texas A&M University. Air samples were also taken at three evenly spaced stations throughout the hypoxic zone to determine *in situ* atmospheric N_2O mixing ratios.

Sample preparation for N_2O analysis consisted of simultaneously removing 5ml of water in the capped vial while injecting N_2 gas to create a headspace of known volume. This was done with two syringes, one empty 5 ml syringe and one glass 50 ml Luer-Lock syringe flushed 3 times with N_2 gas. The weight of the vial was taken before and after water extraction. The vials were shaken on an orbital rotator (Barnstead Lab-line) for 1 hr at room temperature in order for the N_2O to equilibrate with the headspace and for the temperature to equilibrate to room temperature. Samples (0.1 ml) were removed from the headspace with a locking syringe (Hamilton) and injected into the GC for analysis.

Samples were analyzed by gas chromatography (GC) using an Agilent GC-6850 equipped with a 64Ni μ-electron capture detector (μECD) based on the hot ECD method (Rasmussen et al. 1976). The GC was equipped with a 30 m HP Plot/Q capillary column, 0.530 mm wide. The carrier gas (He) flow was kept at a constant pressure of 62.053 kPa, the μECD detector is maintained at 310 ºC and the oven containing the column was maintained at 30 ºC. The makeup gas at the detector (95% Ar, 5% CH_4) was maintained

at 4 ml min^{-1}, He at approximately 8 ml min^{-1}, and the total flow through the detector was 12 ml min^{-1}. The retention time for N_2O was just over 3 min, and there was no need for back-flushing, as the oxygen peak did not overlap with the N_2O peak (Fig. 5).

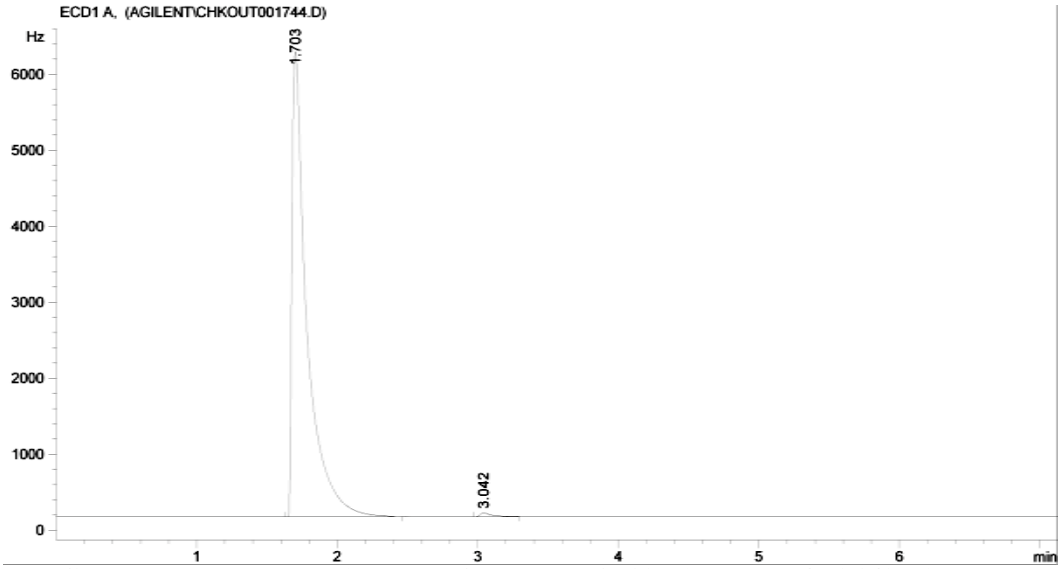

Figure 5. Gas chromatogram showing peaks for oxygen (1.703 min) and N_2O (3.042 min).

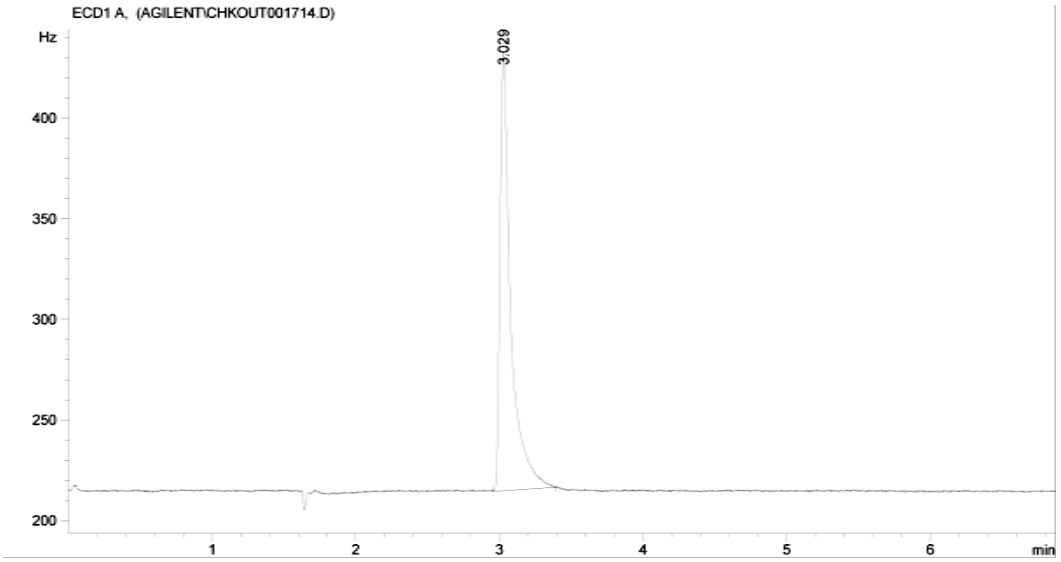

Figure 6. Gas chromatogram for a standard of 0.999 ppbv N_2O in N_2.

Under these conditions, samples were run every 4 minutes without interruptions. N_2O concentrations were compared to a standard of 999 ppbv N_2O in N_2 (Scott Specialty Gases) with an accuracy of ± 2 %. Chromatograms were integrated with Chemstation 62070 software. Measurements were calibrated daily to account for variations in the GC, and to remove impurities column temperatures were ramped up (150 °C) overnight. A representative gas chromatogram for a typical sample is shown in Fig. 5, and the chromatogram for the 0.999 ppbv standard is shown in Fig. 6. An example calibration curve ($r^2 = 0.996$) is shown in Fig. 7,

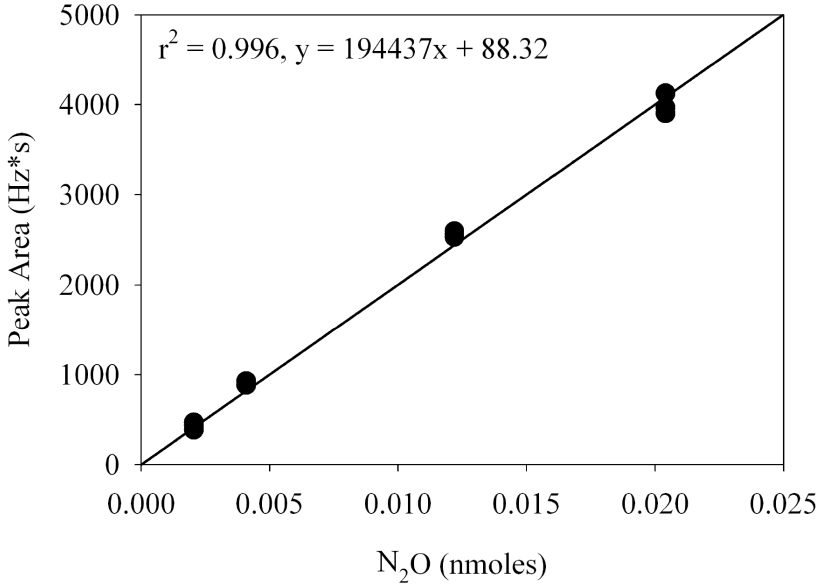

Figure 7. An example N_2O calibration curve using a standard of 0.999 ppbv N_2O in N_2. R^2= 0.996.

During analysis, the temperature and barometric pressure were recorded in the lab in order to account for daily variations. After headspace analysis, vials were filled with pure water and weighed in order to determine the volume of any bubbles that may have occurred in the vial, as well as to get an accurate volume of water extracted.

The dissolved oxygen, *in situ* temperature, and salinity data was obtained from concurrent research conducted on the *R/V Pelican* (Steven DiMarco, pers. comm.) These values, along with peak areas from chromatograms were used to calculate predicted *in situ* N_2O concentrations in the water column, as well as percent saturation. N_2O concentrations were calculated from solubility coefficients corrected for temperature and ssalinity (Weiss & Price 1980). It was important to account for the non-ideality of N_2O because at STP, 1 mole of N_2O occupies ~0.7% less volume than 1 mole of ideal gas (Weiss & Price 1980). Nutrient profiles (NO_3^-, NO_2^-, NH_4^+), oxygen profiles and the physical structure of the water column (i.e. stratification) were used to determine what chemical and physical water column properties affect the distribution of N_2O in the hypoxic zone.

2.3 Storage

Two storage experiments were conducted in order to verify how long samples could be stored without the N_2O concentration changing. Both experiments compared how relatively high concentrations of N_2O in seawater stored vs. relatively low concentrations. During the M11 cruise (April, 2008) field samples were taken from bottom and surface water, which represented the relatively high and low N_2O concentrations respectively. The bottom water was collected from station 1B and the surface water from station BC4. They were not collected from the same station in order to minimize the equilibration time with the air in the Niskin bottle, and because station BC4 was not hypoxic. Approximately 30 replicates were taken from the Niskin bottle

and all were preserved and sealed according to the method previously described. They were then analyzed periodically over 6 months.

In order to account for variability in the field samples, a laboratory storage experiment was also conducted. Previously collected Gulf of Mexico offshore blue water was filtered (0.2 μm) and autoclaved to remove potential organic matter production. For the high N_2O concentration samples, the water was bubbled with N_2O (0.999 ppbv N_2O in N_2 with an accuracy of ±2 %) for one hour. Two triplicate samples were taken immediately: one sealed without formalin and the other with formalin Samples were analyzed immediately to verify the preservative did not effect the N_2O concentration. For the low concentration samples, the seawater was boiled to help drive away dissolved gases, and then bubbled with N_2 gas for one hour. All of the vials (approximately 30 high and 30 low) were preserved, sealed, and stored according to the previously described method and analyzed periodically over 3 months.

2.4 Sediment Incubations

In collaboration with Cifton C. Nunnally (Texas A&M University, Galveston, TX), the sediment-water exchange of N_2O was measured in a batch incubation system on board the *R/V Pelican*. Nitrous oxide fluxes were determined by changes in N_2O concentration in the water overlying the sediment cores incubated under controlled conditions. The objective of these incubations was to determine whether the sediments were a significant source of N_2O to the overlying water. The methods from Nunnally (unpublished) are summarized below.

At stations 8C and 33D, a box core was taken and three subcores with ~15cm overlying water were collected. These cores were capped, placed in a water bath and incubated in the dark with an oxygen electrode threaded through the cap. A rotating magnet prevented stagnation in the outer chamber and cores were allowed to settle until overlying water cleared. The overlying water from each core was sampled for N_2O at 3 time intervals during the incubation in order to see how N_2O concentrations change with decreasing oxygen concentrations. Oxygen values were recorded approximately every hour and nutrient samples were taken each time N_2O samples were taken. Water removed from the core was replaced with bottom water collected from the box core. Rates of N_2O exchange in the sediment were determined by calculating the change in N_2O within the overlying water volume (v) normalized to the surface area of the core (A) and the time of the incubation (t).

$$(\Delta N_2O * v)/(A * t)$$

2.5 Air-Sea Fluxes of Nitrous Oxide

The flux of N_2O to the atmosphere was estimated to test the hypothesis that the Gulf of Mexico hypoxic zone is a significant source of this green house gas. Air-sea gas exchange is driven by a number of factors: wave breaking, wind speed, bubble formation, and molecular and turbulent diffusion. Gas exchange is primarily controlled by wind stress and the Schmidt number, both of which influence the thickness of a stagnant film dominated by molecular diffusivity (Sarmiento and Gruber 2006). Gas transfer velocity calculations for N_2O were made according to Wanninkhof (1992), and flux (F) was estimated using the formula:

$$F = k(C_w - \alpha C_a)$$

Where k is the gas transfer velocity, C_w is the gas concentration in the bulk of the water near the surface, α is the Ostwald solubility coefficient, and C_a is the concentration of gas in the air phase near the interface. The gas transfer velocity (k) is strongly dependent upon wind speed:

$$k_{N2O} = 0.31\ u^2(Sc_{CO2}/Sc_{N2O})^{-1/2}$$

where Sc is the Schmidt number which takes into account deviations of the kinematic viscosity divided by the diffusion coefficients of the gas, and u is the steady wind speed (Wanninkhof 1992, Sweeney et al. 2007). When used outside salinity values of 0 to 35‰ and temperatures of 0 to 30 °C the Schmidt number fit deviates rapidly from the calculated values, and within the range, the uncertainty in the Schmidt number ranges from 3 to 10 % depending upon the gas (Wanninkhof 1992). In order to calculate air-sea gas exchange, shipboard anemometer measurements taken at 17 m were scaled down to 10 m using temperature and relative humidity gradients (Erickson 1993). Ultimately, modeling potential atmospheric flux indicates whether the Gulf of Mexico hypoxic zone is a source of N_2O to the atmosphere.

2.6 Data Analysis

Data was analyzed using Sigmastat 3.1. (Systat Software, Inc.). Analysis of variance (ANOVA) was conducted on data that met the assumptions of normality and equality of variance. For data that did not meet these assumptions, a non-parametric ANOVA was carried out on ranks (Kruskal-Wallis ANOVA). Pair-wise comparisons were made using post-hoc tests. Dunn's pair-wise comparison was used for datasets in

which there were missing data and the Holm-Sidak method was used to make pair-wise comparisons in data where group sizes were equal. Correlation analysis was carried out using the Pearson product moment correlation.

3. RESULTS

3.1 Storage

The four types of samples were significantly different from one another over the storage period (approximately 4 months) ($p < 0.001$), and the samples without formalin were not significantly different from those with formalin ($p = 0.223$). Figure 8 shows changes in N_2O concentration over the storage time; the y-axis range is extended to 30 μmol m^{-3} to show samples relative to the overall cruise mean ± SD. The low concentration samples had the most change ($r^2 = 0.91$), and the bottom samples had the least change ($r^2 = 0.05$). However, overall there was no significant difference between sample storage times ($F_{3, 44} = 72.23$) (Fig. 8).

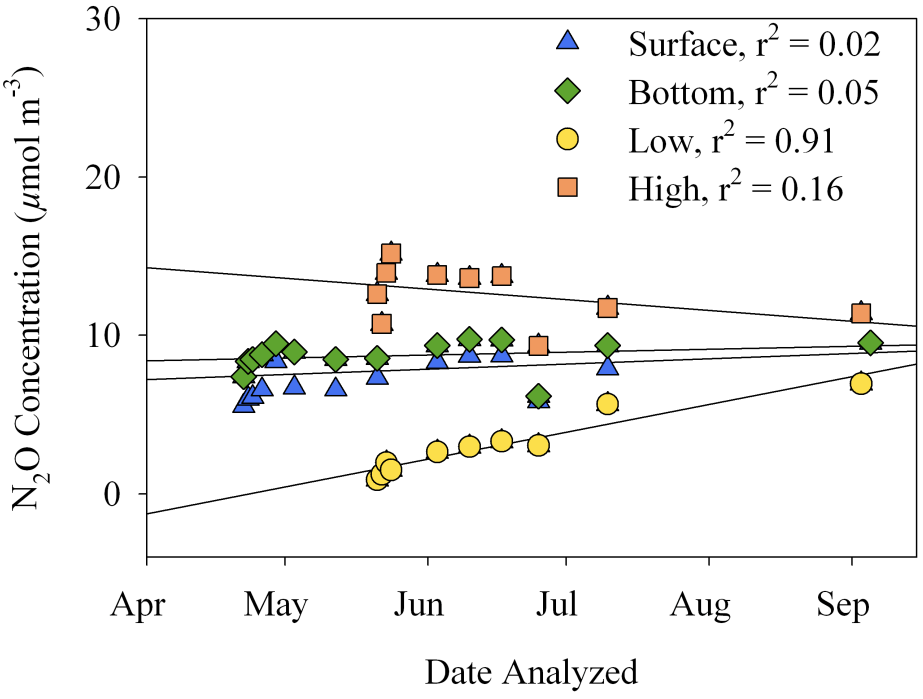

Figure 8. Changes in N_2O concentration over the storage time for 4 treatments (surface and bottom treatments are from the field storage experiment, and low and high treatments are from the lab storage experiment). r^2 values are displayed on the plot.

3.2 Sediment Incubations

For all cruises pooled, there was a significant negative correlation between N_2O and O_2 concentration ($p < 0.05$, $r = -0.341$, $n = 47$) in the water overlying the sediments. As oxygen was consumed during incubation, and nutrients were not added to the chambers, N_2O flux rates for the sediment at stations 8C and 33D were highly variable within cruises and between cruises. For M10 (September 2007) station 8C, as O_2 concentration decreased from 1.04 to 0.10 ml l^{-1} over 25 h, N_2O concentration decreased from 11.84 to 8.67 μmol m^{-3} (Fig. 9A). For station 33D, O_2 decreased from 0.54 to 0.34 ml l^{-1} over 16.5 h, while N_2O increased from 10.31 to 11.02 μmol m^{-3} (Fig. 9B). The flux for the sediments at 8C and 33D were -7.30 ± 8.34 μmol m^{-2} d^{-1} (± SD) and 0.07 ± 0.05 μmol m^{-2} d^{-1} respectively.

For the M11 (April 2008), station 8C sediment O_2 concentration decreased from 3.99 to 1.23 ml l^{-1} while N_2O concentrations increased from 5.80 to 7.40 μmol m^{-3} over a 33 h incubation time (Fig. 9C). Flux rate for the sediment was 0.08 ± 0.03 μmol m^{-2} $d^{-1.}$

The M12 (July 2008) cruise sediment O_2 concentration for station 8C decreased from 1.19 to 0.58 ml l^{-1} and N_2O concentration decreased from 14.48 to 8.09 μmol m^{-3} over a 19 h incubation time (Fig. 9D). Flux rate for the sediment was -1.12 ± 1.14 μmol m^{-2} $d^{-1.}$ For station 33D, over 18 h, O_2 decreased from 0.80 to 0.06 ml l^{-1}, while N_2O decreased from 13.30 to 7.45 μmol m^{-3} (Fig. 9E). The sediment flux rate was -0.63 ± 0.17 μmol m^{-2} d^{-1}.

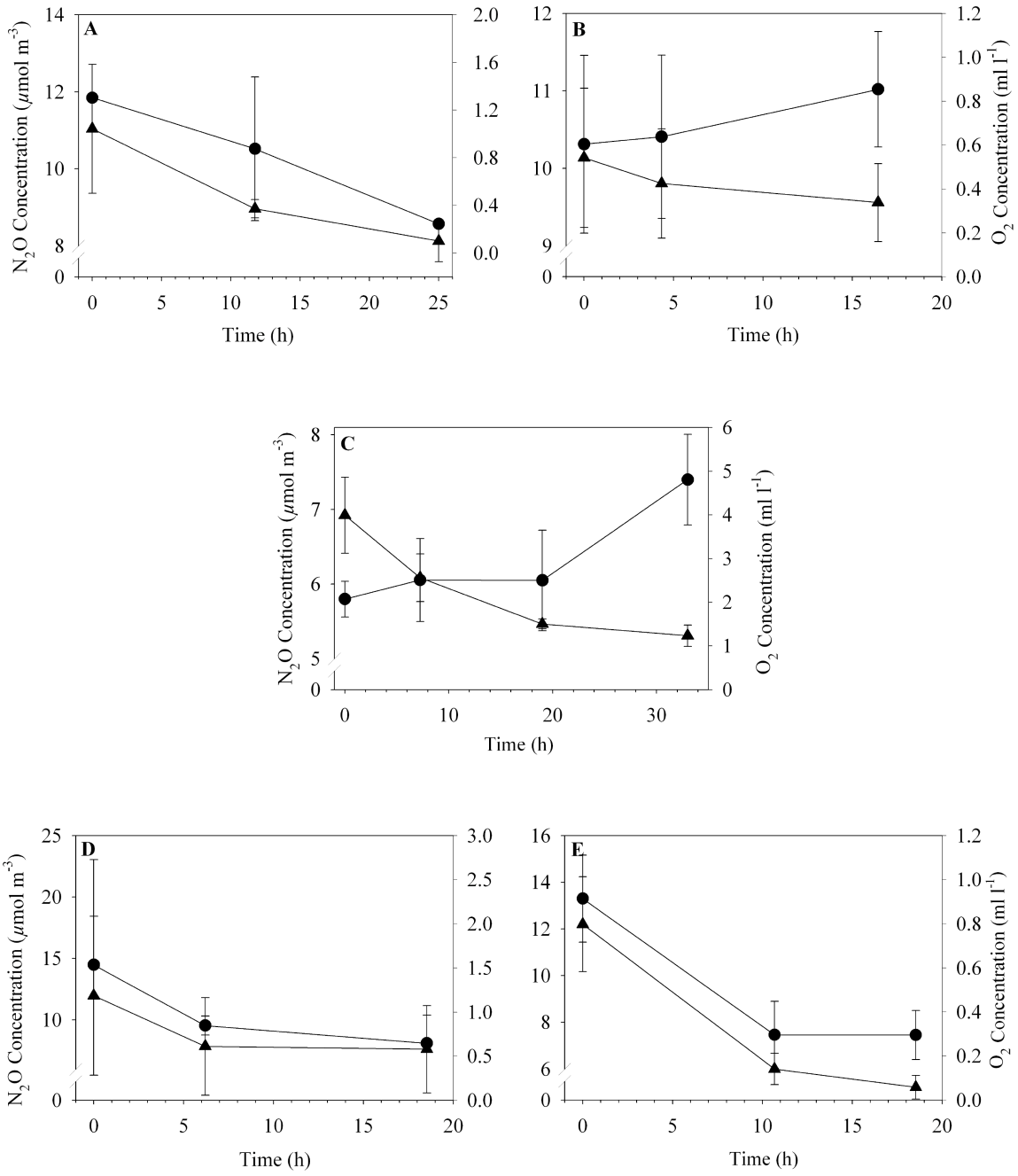

Figure 9. Concentrations of N_2O (circles) and O_2 (triangles) in the water overlying sediment incubations (A) M10 (September 2007) station 8C, (B) M10 (September 2007) station 33D, (C) M11 (April 2008) station 8C, (D) M12 (July 2008) station 8C, and (E) M12 (July 2008) station 33D. Bars represent mean ± S.D.

3.3 Combined Stations and Depths

For all three cruises, the range of N_2O was 4.72 to 182.74 μmol m^{-3} for all the depths sampled and for every station. Water column concentrations of N_2O for M10 (September 2007) ranged from 7.88 to 62.39, with a mean of 20.85 ± 13.02 (± SD) μmol m^{-3}. Associated water column saturations ranged from 83 to 1084 %, with an average of 343 ± 228 %. Hypoxia (O_2 < 1.4 ml l^{-1}) occurred in 7 of the 11 stations (3B, 13B, 8C, 9C,10C, 11C, 33D).

During the M11 (April 2008) cruise, N_2O concentrations ranged from 5.74 to 17.45 μmol m^{-3}, with a mean of 7.16 ± 1.54 μmol m^{-3}. Water column N_2O saturation ranged from 72 to 238 %, with a mean of 96 ± 22 %. No stations were found to be hypoxic, but several stations have missing O_2 data.

During the M12 (July 2008) cruise, N_2O concentrations ranged from 4.72 to 182.74 μmol m^{-3} with a mean concentration of 16.14 ± 26.55 μmol m^{-3}. N_2O saturations ranged from 69 to 2878 %, with a mean of 256 ± 419 %. Hypoxia occurred in at least 12 of the 17 stations sampled (7B, 8B, BC1, BC3, BC4, 7C, 8C, 9C, 26D, 28D, 33D, 37D), two stations had missing O_2 data (38D, 41D).

When the data for all three cruises was pooled together, N_2O concentration positively correlated with salinity, ($p < 0.001$, $r = 0.211$, $n = 630$) and temperature ($p < 0.001$, $r = 0.226$, $n = 630$) and negatively correlated with water column oxygen concentration ($p < 0.001$, $r = -0.197$, $n = 552$). The strongest positive correlation was between salinity and depth ($p < 0.001$, $r = 0.718$, $n = 632$), and the strongest negative correlation was between O_2 and NO_2^- ($p < 0.001$, $r = -0.509$, $n = 553$). All three cruises

were statistically different from one another with respect to N_2O concentration ($H = 293$, $p < 0.001$, 2 degrees of freedom).

Scatter plots show the relationship between N_2O concentration and temperature, salinity, O_2, NO_3^-, NO_2^- and NH_4^+ (Figs. 10, 11, and 12), and distinct differences can be seen between cruises. The M11 (April 2008) shows low and narrow ranges of N_2O associated with a weak pycnocline, low temperature and salinity, low nutrient concentrations, and higher O_2 concentrations.

The M12 (July 2008) shows that high N_2O concentrations were associated with the base of the pycnocline, as well as with low O_2 and high nutrient concentrations. Saturations were highest at 10 m, which was the depth of the pycnocline and oxycline (Fig. 11A). High N_2O concentrations were also associated with high water column DIN (Fig. 12B), and the ratio of N_2O to NO_2^- increases with increasing oxygen concentration and decreasing depth (Figs. 12A, and 12C).

The M10 (September 2007) fell between these two scenarios; there were high temperatures and salinities but not as strong water stratification as the M12. N_2O concentrations were mid-range and did not exhibit differences with depth (Fig. 11A). NO_2^- concentrations are high near the bottom (Fig. 12F).

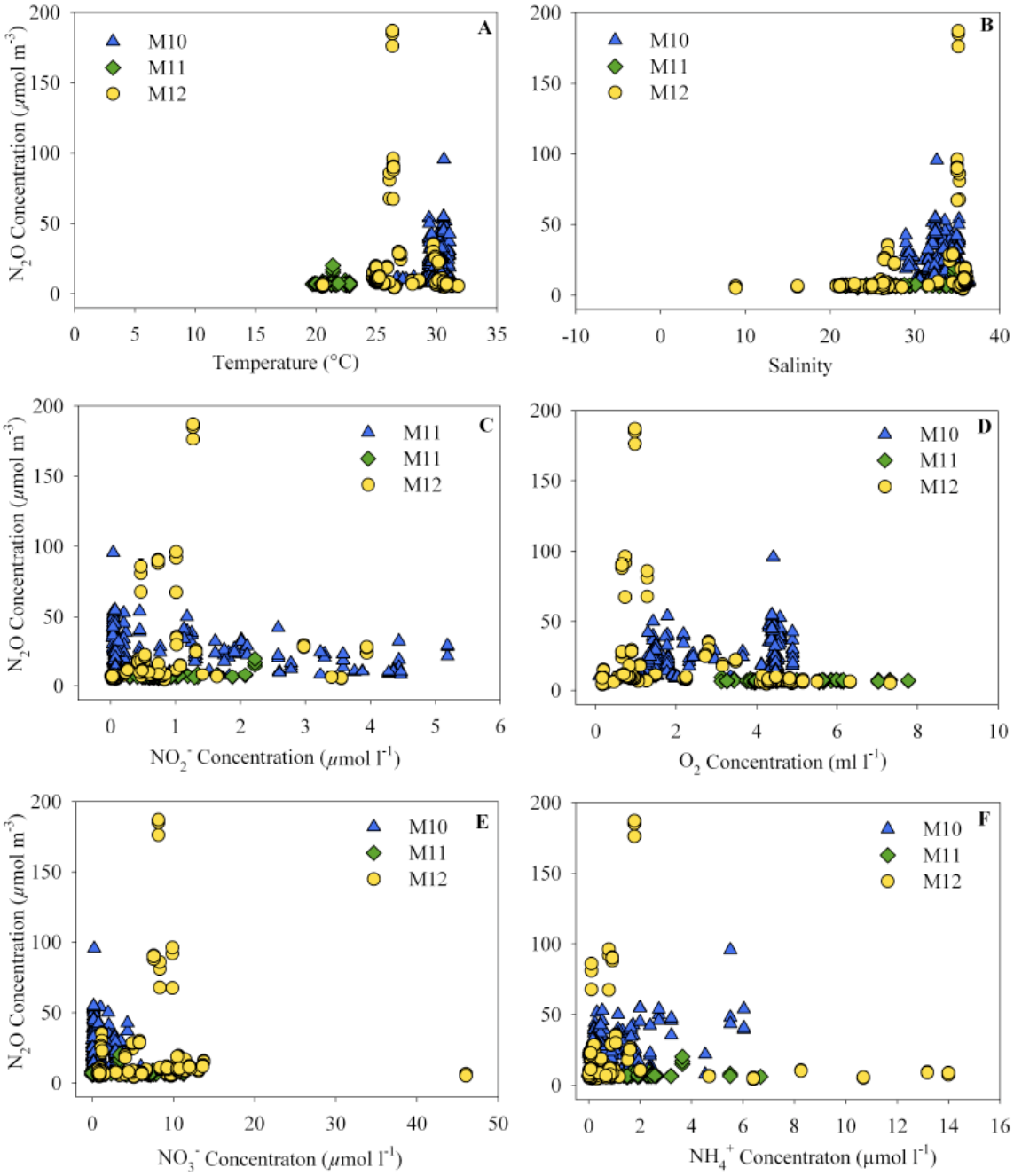

Figure 10. Relationship between N_2O concentration and (A) temperature, (B) salinity, (C) NO_2^- concentration, (D) O_2 concentration, (E) NO_3^- concentration, and (F) NH_4^+ concentration for the M10 (September 2007), M11 (April 2008), and M12 (July 2008).

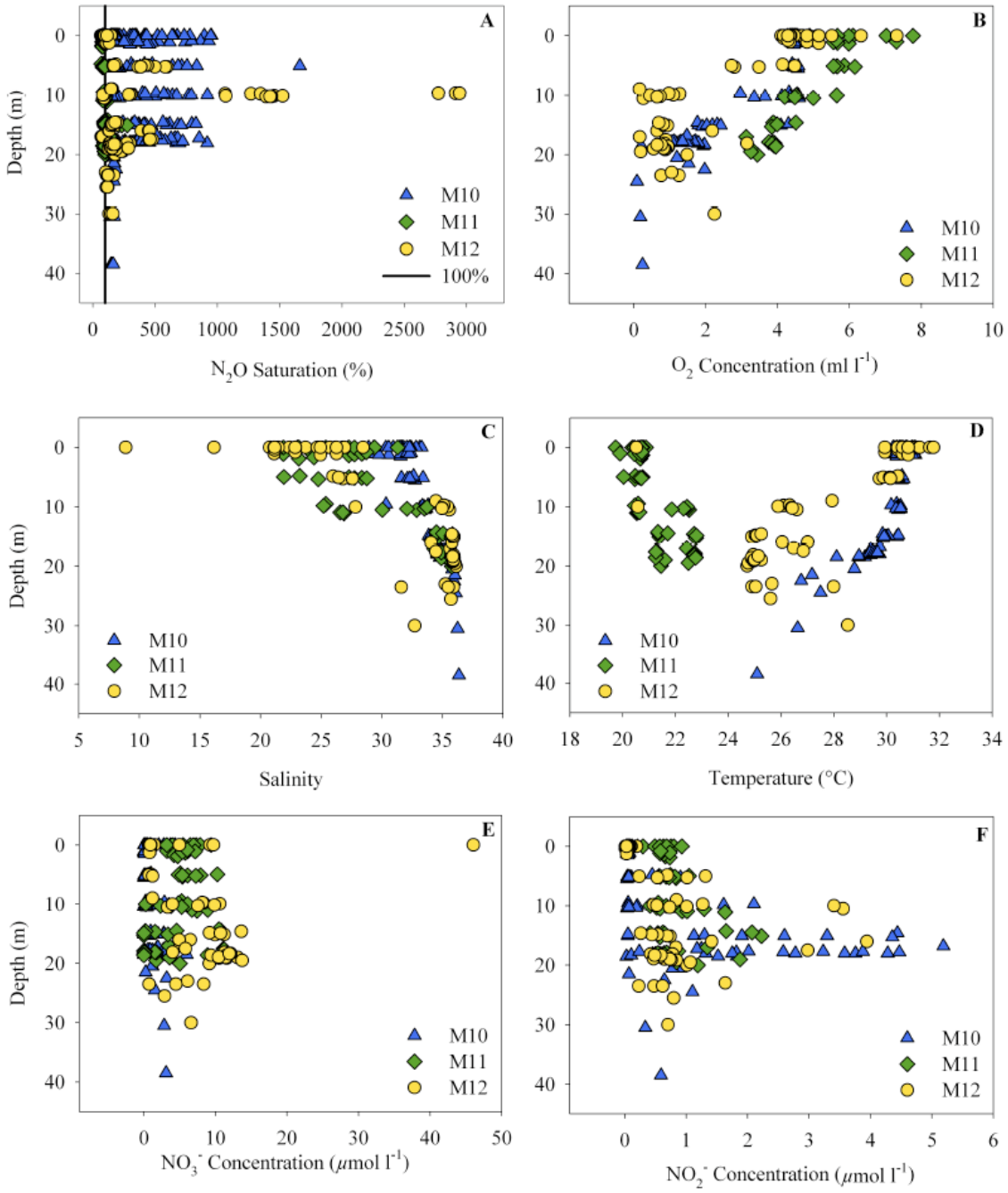

Figure 11. Relationship between depth and (A) N_2O saturation (line indicates 100% saturation), (B) O_2 concentration, (C) salinity, (D) temperature, (E) NO_3^- and (F) NO_2^- for M10 (September 2007), M11 (April 2008), and M12 (July 2008).

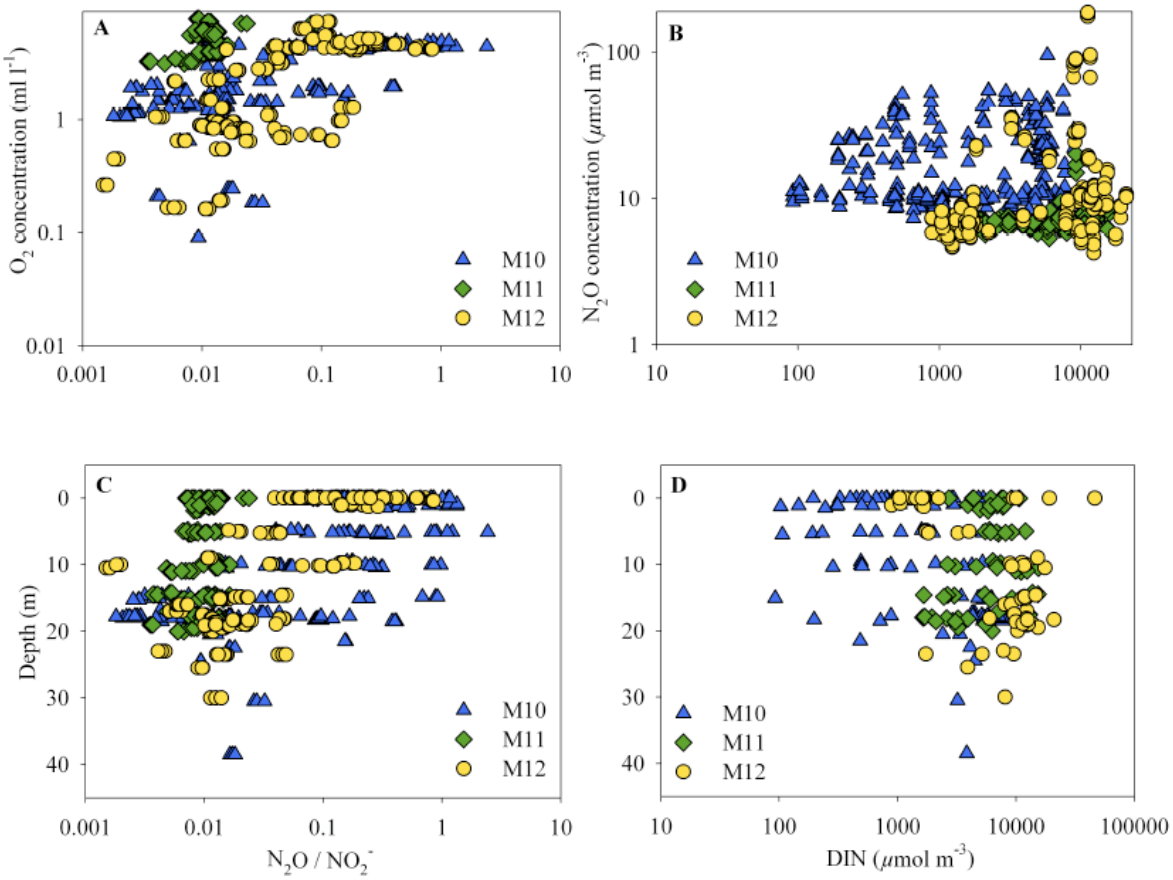

Figure 12. Relationship between (A) O_2 concentration (log_{10}) and the ratio of N_2O to NO_2^- (log_{10}), (B) N_2O (log_{10}) and DIN (log_{10}), (C) depth and the ratio of N_2O to NO_2^- (log_{10}), and (D) depth and DIN.

3.4 Water Column

Typical vertical distributions of N_2O, O_2, temperature, salinity, NH_4^+, NO_3^-, and NO_2^- are shown for each cruise in Figs. 13, 14, and 15. All vertical profiles came from the station 8C time series with the exception of M11 (April 2008) stations 1B, 4B, and 7B. M10 (September 2007) vertical distributions of N_2O were generally more variable with larger standard deviations associated with each depth (Fig. 13). N_2O concentrations ranged from 8.53 to 62.34 μmol m^{-3}, saturations ranged from 147 to 1084 %, and generally fell between values from the M11 and M12 cruises. Temperatures ranged from

29 to 31 ºC, salinity ranged from 29 to 36, oxygen concentrations reached as low as 1.05 ml l^{-1}, and hypoxia occurred in 5 of the 10 sampling times. There was not a significant difference between depths with respect to N_2O concentration. NO_3^- concentrations ranged from 0.003 to 4.329 μmol l^{-1}, NO_2^- from 0.02 to 5.19 μmol l^{-1}, and NH_4^+ from 0.004 to 6.037 μmol l^{-1}. See Appendix A for the remaining vertical profiles from the M10.

M11 (April 2008) N_2O concentrations were well mixed throughout the water column and all values were relatively low (Fig. 14). N_2O concentration ranged from 5.74 to 17.45 μmol m^{-3}, and associated saturations ranged from 71 to 238 %. Temperature ranged from 20 to 23 ºC and salinity ranged from 22 to 36 indicating there was a weak thermocline but strong halocline. Oxygen concentrations that were recorded were not below 3.76 ml l^{-1} (several missing values). NO_3^- concentrations ranged from 0.002 to 11.220 μmol l^{-1}, NO_2^- from 0.411 to 2.22 μmol l^{-1}, and NH_4^+ from 3.76 to 6.15 μmol l^{-1}. Depths were significantly different from one another with respect to N_2O concentration ($H = 17.13$, $p < 0.01$, 5 degrees of freedom), specifically when comparing the bottom and surface concentrations. See Appendix A for the remaining M11 profiles.

The M12 (July 2008) vertical distributions generally had a large spike in N_2O around 10m associated with the base of the pycnocline and oxycline (Fig. 15). The water was highly stratified with a well-defined pycnocline. N_2O concentrations ranged from 6.43 to 182.74 μmol m^{-3} with associated saturations of 107 to 2878 %. The spike in N_2O at 10 m was associated with a saturation of 2878 %, which was the highest concentration recorded from all three cruises (Fig. 15). Temperatures ranged from 25 to 31ºC, salinities ranged from 21 to 36, and oxygen concentrations reached as low as 0.645 ml l^{-1}. NO_3^-

concentrations ranged from 0.75 to 13.61 μmol l^{-1}, NO_2^- from 0.008 to 1.313 μmol l^{-1}, and NH_4^+ from 0.005 to 6.254 μmol l^{-1}. Depths were statistically different from one another with respect to N_2O ($H = 82.61$, $P < 0.001$, 5 degrees of freedom).

3.5 Bottom and Surface Stations

Where full water column profiles were not taken, bottom and surface samples were collected. Nearly every station (with the exception of the 8C time series and M11 stations 1B, 4B, and 7B) had only bottom and surface samples. This section does not take into account water column profiles or time-series data (see 3.4). M10 (September 2007) bottom and surface N_2O concentrations ranged from 7.59 to 24.69 μmol m^{-3}, the mean N_2O concentration at the bottom was 9.95 ± 1.07 (± SD) μmol m^{-3} and on the surface it was 10.65 ± 2.97 μmol m^{-3}. Mean saturations at the bottom and surface were 162 ± 16 % and 184 ± 51 % respectively (Fig. 16A). Temperature ranged from 25 to 31 ºC, salinity ranged from 30 to 36, and oxygen concentration fell to 0.09 ml l^{-1}. There was no significant difference between the bottom and surface with respect to N_2O concentration.

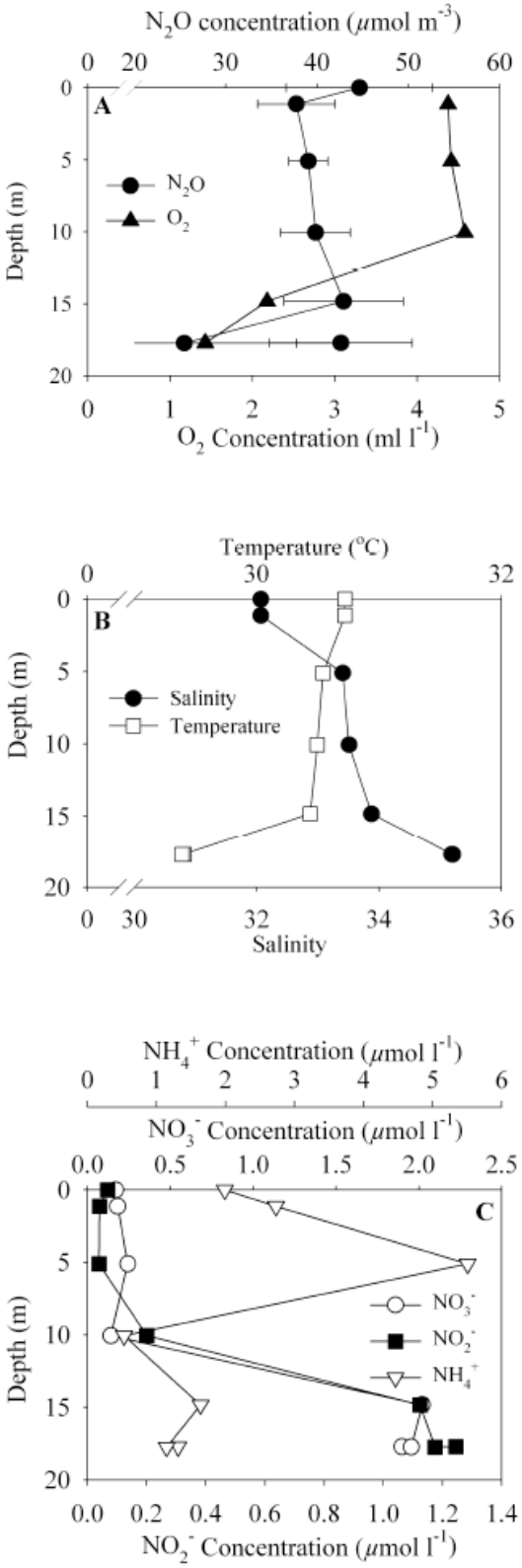

Figure 13. M10 (September 2007 4:00 AM CST) station 8C depth profiles for (A) N_2O and O_2, (B) temperature and salinity, and (C) NO_3^-, NO_2^- and NH_4^+. Bars represent mean ± S.D.

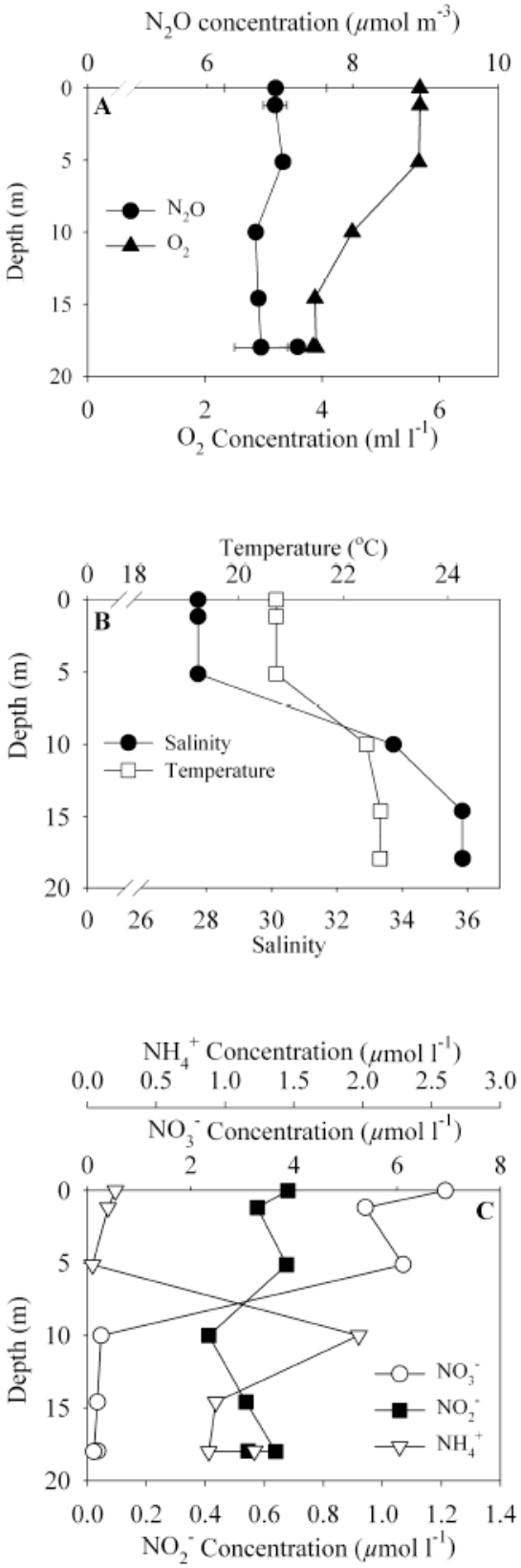

Figure 14. M11 (April 2008 4:00 AM) station 8C depth profiles for (A) N_2O and O_2, (B) temperature and salinity, and (C) NO_3^-, NO_2^- and NH_4^+. Bars represent mean ± S.D.

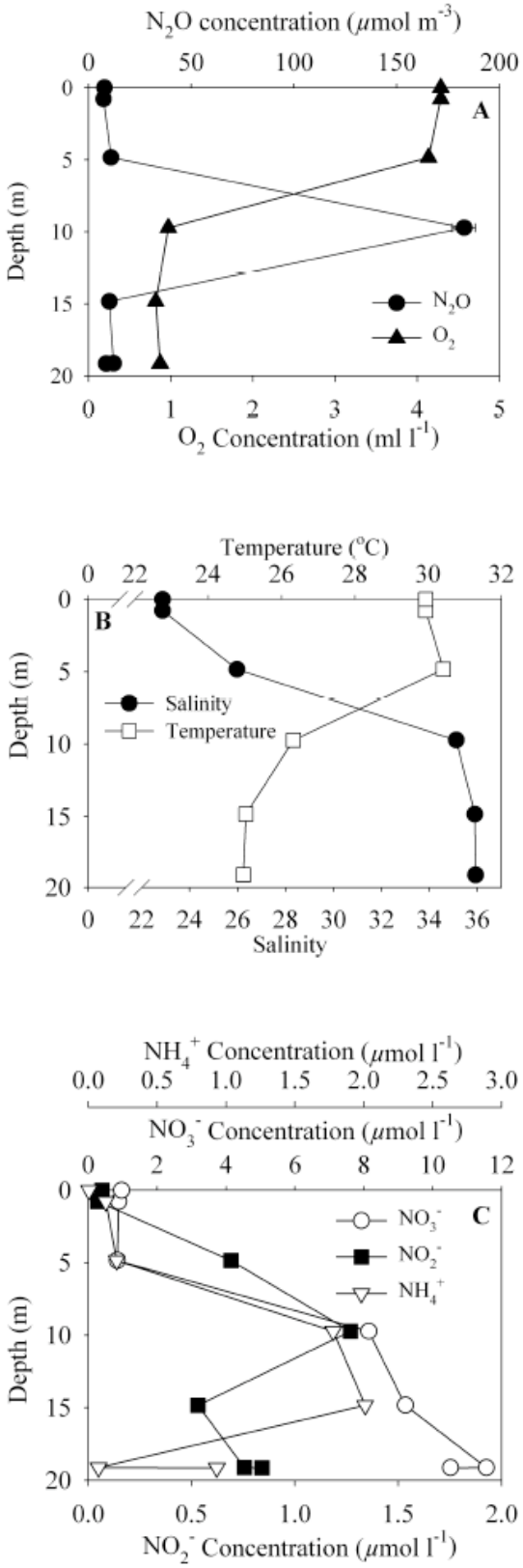

Figure 15. M12 (July 2008 8:00 AM) station 8C depth profiles for (A) N_2O and O_2, (B) temperature and salinity, and (C) NO_3^-, NO_2^- and NH_4^+. Bars represent mean ± S.D.

M11 (April 2008) bottom and surface N_2O concentration ranged from 6.27 to 9.54 μmol m^{-3}, with a bottom mean of 7.10 ± 0.70 μmol m^{-3} and a surface mean of 6.88 ± 0.40 μmol m^{-3}. Mean saturation at the bottom was 98 ± 11 % and at the surface it was 87 ± 5 % (Fig. 16B). Temperature ranged from 20 to 23 ºC, salinity ranged from 23 to 36, and recorded oxygen concentration did not go below 3.125 ml l^{-1} (several missing values). There was no significant difference between the bottom and surface with respect to N_2O concentration.

M12 (July 2008) bottom and surface N_2O concentrations ranged from 4.25 to 30.02 μmol m^{-3}, with a bottom mean of 11.00 ± 6.95 μmol m^{-3} and a surface mean of 6.26 ± 0.93 μmol m^{-3}. Mean saturation at the bottom and surface was 171 ± 111 and 103 ± 17 % respectively (Fig. 16C). Temperatures ranged from 21 to 32 ºC, salinities ranged from 9 to 36, and oxygen concentrations fell to 0.162 ml l^{-1} (Fig. 16C). There was a significant difference between the bottom and surface with respect to N_2O concentration ($H = 34.795$, $p < 0.001$, 1 degree of freedom). A Summary of all water column, surface, and bottom ranges reported is presented in Table 2.

Table 2. Ranges of N_2O, temperature, salinity O_2, NO_3^-, NO_2^- and NH_4^+ in the water column, bottom, and surface for the M10 (September 2007), M11 (April 2008), and M12 (July 2008). Water Column includes the bottom and surface.

Cruise	Depth	N_2O (μmol m^{-3})	N_2O Saturation (%)	Temp. (°C)	Salinity	O_2 (lower limit) (ml l^{-1})	NO_3^- (μmol l^{-1})	NO_2^- (μmol l^{-1})	NH_4^+ (μmol l^{-1})
M10	Water Column	8.53 to 62.34	147 to 1084	29 to 31	29 to 36	1.05	0.003 to 4.33	0.02 to 5.19	0.004 to 6.04
	Bottom	7.59 to 11.87	128 to 196	25 to 30	30 to 36	0.09	0.245 to 5.98	0.054 to 1.83	0.04 to 1.84
	Surface	8.44 to 24.69	146 to 427	30 to 31	30 to 33	4.27	0.09 to 2.78	0.03 to 0.09	0.03 to 2.40
M11	Water Column	5.74 to 17.45	71 to 238	20 to 23	22 to 36	3.76	0.002 to 11.22	0.41 to2.22	3.76 to 6.15
	Bottom	6.53 to 9.54	86 to 134	21 to 23	25 to 36	3.13	1.68 to 5.28	0.54 to 1.88	0.04 to 2.36
	Surface	6.27 to 7.55	80 to 99	20 to 21	23 to 31	6.10	0.99 to 7.87	0.08 to 0.80	0.01 to 2.63
M12	Water Column	6.43 to 182.74	107 to 2878	25 to 31	21 to 36	0.65	0.75 to 13.61	0.01 to 1.31	0.01 to 6.25
	Bottom	4.25 to 30.02	67 to 477	20 to 29	28 to 36	0.02	0.75 to 13.73	0.23 to 3.94	0.07 to 13.17
	Surface	4.63 to 8.96	64 to 151	21 to 31	9 to 28	4.10	0.68 to 46.02	0.01 to 0.19	0.02 to 13.99

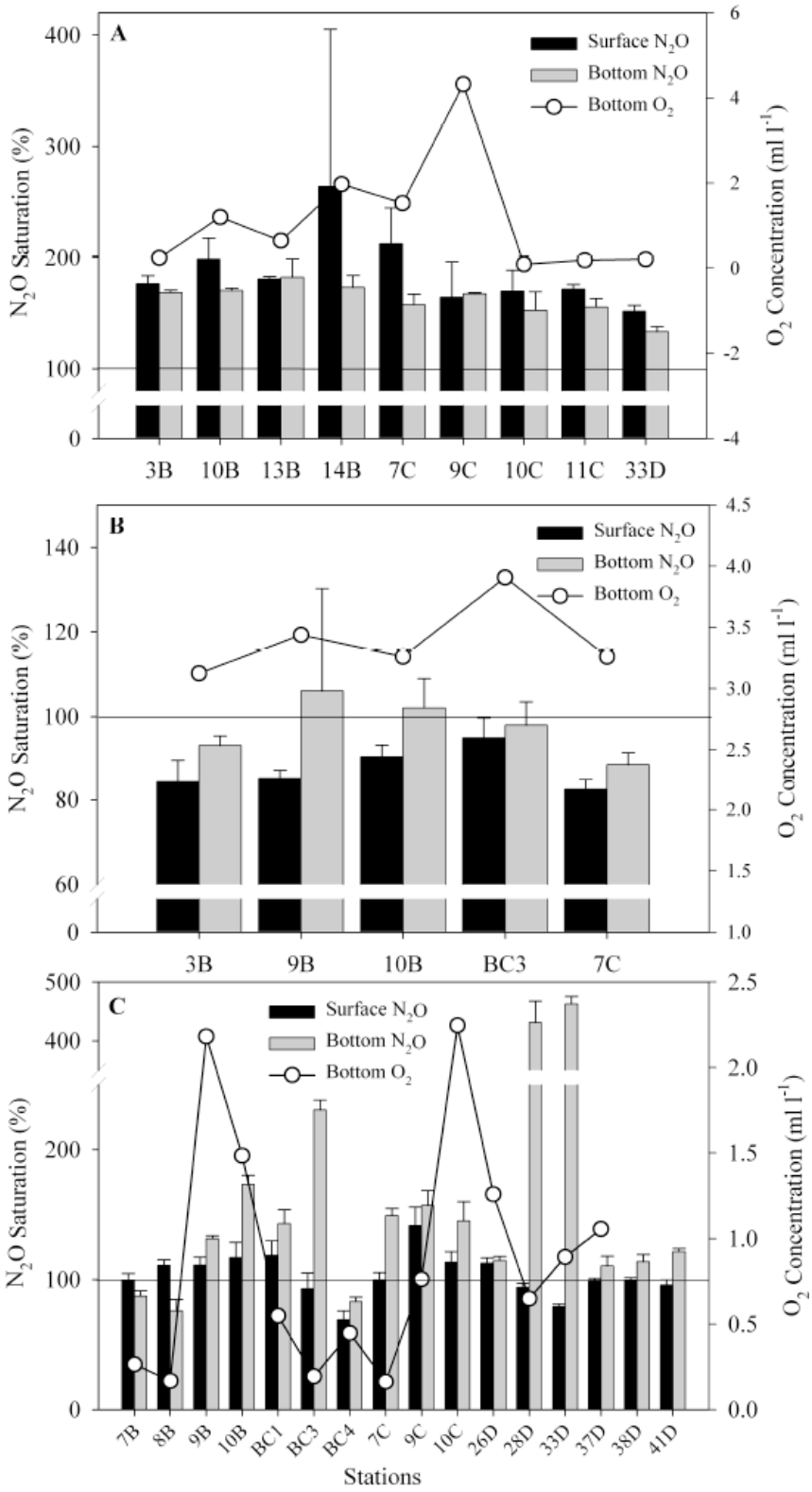

Figure 16. N_2O saturations (%) for each station at the surface (black) and bottom (grey) for (A) M10 (September 2007), (B) M11 (April 2008), and (C) M12 (July 2008). Bottom O_2 concentration is plotted over the bar graphs. Horizontal line indicates 100% saturation. Note the difference in scales for each graph. Bars represent mean ± S.D.

3.6 Surface Saturations and Fluxes

The N_2O concentrations in surface waters were generally supersaturated, i.e. above the concentrations expected from equilibrium with the air during the two summer cruises, and undersaturated during the spring cruise. Figures 17, 18, and 19 show the geographic distribution of surface saturations for each cruise. Surface waters were generally more saturated with N_2O at sites between the mouths of the Mississippi Atchafalaya Rivers (zone B) compared with western sites (zones C and D). The M10 (September 2007) and had only positive fluxes of N_2O to the atmosphere, the M11 (April 2008) had nearly all negative fluxes with the exception of one zero value, and M12 (July 2008) had mostly positive and some low negative fluxes (Table 3). A summary of the major variables used in the flux calculations can be found in Tables 3 and 4. Overall, wind speeds were variable and were one of the major factors contributing to the flux of N_2O.

Surface saturations for M10 (Sept. 2007) ranged from 152 to 441 %, with a mean of 213 ± 86 % (Fig. 17). This was associated with a high rate of emission to the atmosphere (30.37 to 153.22 μmol m^{-2} d^{-1}; with a mean of 166.41 ± 46.62 (± SD) μmol m^{-2} d^{-1}).

Surface saturations for M11 (April 2008) were all below 100 %, ranging from 75 to 95 %, with a mean of 86 ± 6 % (Fig. 18). The associated atmospheric emissions ranged from -11.27 to 0.00 μmol m^{-2} d^{-1}; average -5.13 ± 3.96 μmol m^{-2} d^{-1}.

The M12 (July 2008) surface saturations ranged from 69 to 142 % with an average of 104 ± 17 % (Fig. 19) and associated emissions ranged from -3.05 to 44.02 μmol m^{-2} d^{-1}; with an average of 8.45 ± 12.69 μmol m^{-2} d^{-1}.

Table 3. Surface N_2O concentrations, saturations, wind speeds (at 10m), and atmospheric fluxes for M10 (Sept. 2007), M11 (April 2008) and M12 (June 2008). *Temperatures above 30 °C exceed flux model parameters, **station 8C values are means from 12 to36 hr periods (see Table 4).

Cruise	Station & Time	Temp (°C) *	Salinity	N_2O concentration (μmol m^{-3})	N_2O Saturation (%)	Wind Speed (m s^{-1})	Flux (μmol m^{-2} d^{-1})
M10	3B	30.7	32.8	10.11 ± 0.43	176 ± 7	6.85	20.56
M10	10B	31.0	31.6	11.39 ± 1.09	198 ± 19	9.22	48.01
M10	13B	30.8	31.4	10.42 ± 0.13	181 ± 2	12.61	73.93
M10	14B	30.8	30.9	15.25 ± 8.18	264 ± 141	12.88	153.22
M10	7C	30.4	30.3	12.44 ± 1.88	212 ± 32	11.67	87.26
M10	8C**	30.7	30.9	25.63 ± 15.07	441 ± 259	8.75	135.74
M10	9C	30.5	31.7	9.52 ± 1.84	164 ± 32	12.52	58.57
M10	10C	30.5	33.1	9.79 ± 1.07	170 ± 19	8.02	25.84
M10	11C	30.6	33.3	9.84 ± 0.24	172 ± 4	8.60	30.37
M10	33D	30.4	31.3	8.85 ± 0.30	152 ± 5	10.01	30.61
Mean ± S.D.				**12.32 ± 5.03**	**213 ± 86**	**10.11 ± 2.16**	**66.41 ± 46.62**
M11	1B	20.6	24.4	5.92 ± 0.18	75 ± 2	0.04	0.00
M11	3B	20.4	29.4	6.53 ± 0.42	84 ± 5	11.81	-10.62
M11	4B	20.7	23.2	6.47 ± 0.38	81 ± 5	5.00	-2.35
M11	7B	20.5	21.9	6.85 ± 0.35	86 ± 4	5.77	-2.44
M11	9B	19.7	23.0	6.97 ± 0.15	85 ± 2	12.43	-11.27
M11	10B	19.9	24.3	7.30 ± 0.22	91 ± 3	11.29	-5.43
M11	BC3	20.9	31.3	7.19 ± 0.36	95 ± 5	10.22	-1.48
M11	7C	20.6	25.4	6.49 ± 0.21	83 ± 3	8.47	-6.27
M11	8C**	20.7	28.0	7.00 ± 0.39	92 ± 6	13.45	-6.31
Mean ± S.D.				**6.75** ± 0.43	**86 ± 6**	**8.72 ± 4.37**	**-5.13 ± 3.96**
M12	7B	30.8	16.2	6.18 ± 0.32	100 ± 5	6.90	1.09
M12	8B	31.0	20.8	6.71 ± 0.25	111 ± 4	10.27	9.44
M12	9B	31.1	23.7	6.60 ± 0.37	111 ± 6	8.26	6.04
M12	10B	30.6	22.4	7.08 ± 0.72	117 ± 12	7.50	6.78
M12	BC1	31.1	21.4	7.12 ± 0.68	119 ± 11	6.24	5.15
M12	BC3	30.4	8.9	6.04 ± 0.79	93 ± 12	13.28	-3.05
M12	BC4	20.5	26.8	5.40 ± 0.54	69 ± 7	0.75	-0.09
M12	7C	30.7	26.2	5.97 ± 0.33	100 ± 6	3.19	0.28
M12	8C**	30.4	23.3	7.28 ± 1.03	120 ± 18	7.35	44.02
M12	9C	30.7	26.2	8.39 ± 0.84	142 ± 14	8.06	16.75
M12	10C	30.6	26.9	6.72 ± 0.49	113 ± 8	6.21	3.80
M12	26D	31.2	25.0	6.63 ± 0.24	113 ± 4	5.74	3.19
M12	28D	31.3	25.0	5.54 ± 0.19	94 ± 3	8.95	-0.65
M12	33D	30.6	26.2	4.72 ± 0.11	79 ± 2	3.15	-0.91
M12	37D	30.8	24.7	5.89 ± 0.13	99 ± 2	3.60	7.26
M12	38D	31.6	28.5	5.68 ± 0.14	99 ± 3	4.27	10.14
M12	41D	31.8	25.7	5.54 ± 0.23	96 ± 4	7.93	34.34
Mean ± S.D.				**6.32 ± 0.88**	**104 ± 17**	**6.57 ± 3.01**	**8.45 ± 12.69**

The N_2O values for station 8C are listed in Table 4 as μmol m^{-2} h^{-1} rather than μmol m^{-2} d^{-1} because sampling occurred every four hours. However, the flux values from

station 8C that are incorporated into Table 4 are means in μmol m^{-2} d^{-1}. Figure 20 shows how surface saturation changes over time. Over a 36 hr time period, M10 station 8C N_2O saturations ranged from 147 to 761 % with a mean of 441 ± 259 % and fluxes ranged from 1.56 to 14.81 μmol m^{-2} h^{-1} with a mean of 5.66 ± 5.10 μmol m^{-2} h^{-1}. During the M11 (April 2008) cruise, over the course of 12 hours station 8C N_2O saturations ranged from 84 to 96 % with a mean of 92 ± 6 % and fluxes ranged from -0.37 to -0.10 μmol m^{-2} h^{-1} with a mean of -0.26 ± 0.12 μmol m^{-2} h^{-1}. N_2O saturations for the M12 station 8C ranged from 107 to 149 % with a mean of 120 ± 18 % and fluxes ranged from 0.00 to 2.47 μmol m^{-2} h^{-1} with a mean of 1.83 ± 1.05 μmol m^{-2} h^{-1}.

Table 4. Surface N_2O concentrations, saturations, wind speeds (at 10m), and atmospheric fluxes over time for M10 (Sept. 2007), M11 (April 2008) and M12 (June 2008) station 8C. *Temperatures above 30 exceed flux model parameters (see text).

Cruise	Station & Time	Temp (°C) *	Salinity	N_2O concentration (μmol m-3)	N_2O Saturation (%)	Wind Speed (m s^{-1})	Flux (μmol m^{-2} h^{-1})
M10	8C 12am	31.1	30.6	10.62 ± 0.63	186 ± 11	9.53	1.86
M10	8C 4am	30.7	32.1	44.65 ± 8.02	761 ± 137	9.78	14.81
M10	8C 8am	31	29.4	51.51 ± 5.73	892 ± 99	6.17	6.98
M10	8C 12pm	30.5	31.4	19.73 ± 3.57	342 ± 62	4.08	0.93
M10	8C 4pm	31	28.9	39.78 ± 4.02	685 ± 69	3.21	1.41
M10	8C 8pm	31	29.5	24.84 ± 4.95	428 ± 85	10.78	8.94
M10	8C 12am	30.4	31.6	25.07 ± 6.93	430 ± 119	12.96	12.77
M10	8C 4am	30.3	31.6	21.56 ± 3.17	369 ± 54	9.5	5.61
M10	8C 8am	30.2	32.1	10.05 ± 0.47	173 ± 8	9.48	1.56
M10	8C 12pm	30.4	32.3	8.52 ± 0.16	147 ± 3	12.03	1.68
Mean ± S.D.				**25.63 ± 15.07**	**441.4 ± 259**	**8.75 ± 3.24**	**5.66 ± 5.10**
M11	8C 12am	20.7	27.3	7.37 ± 0.46	95 ± 6	12.93	-0.10
M11	8C 4am	20.7	27.8	6.94 ± 0.70	96 ± 5	11.7	-0.26
M11	8C 8am	20.6	28.4	6.48 ± 0.58	84 ± 7	9.89	-0.32
M11	8C 12pm	20.7	28.7	7.19 ± 0.35	93 ± 5	19.29	-0.37
Mean ± S.D.				**7.00 ± 0.39**	**92.1 ± 6**	**13.4 ± 4.09**	**-0.26 ± 0.12**
M12	8C 12am	30.7	21.1	6.79 ± 0.26	112 ± 4	8.86	2.10
M12	8C 4am	30.4	21.2	6.53 ± 0.05	107 ± 1	9.96	2.53
M12	8C 8am	29.9	22.9	7.78 ± 0.77	127 ± 13	0.29	0.00
M12	8C 12pm	29.9	26.3	8.85 ± 0.19	149 ± 3	7.79	2.07
M12	8C 8pm	30.8	24.9	6.43 ± 0.60	108 ± 10	9.85	2.47
Mean ± S.D.				**7.28 ± 1.03**	**120.4 ± 18**	**7.35 ± 4.04**	**1.83 ± 1.05**

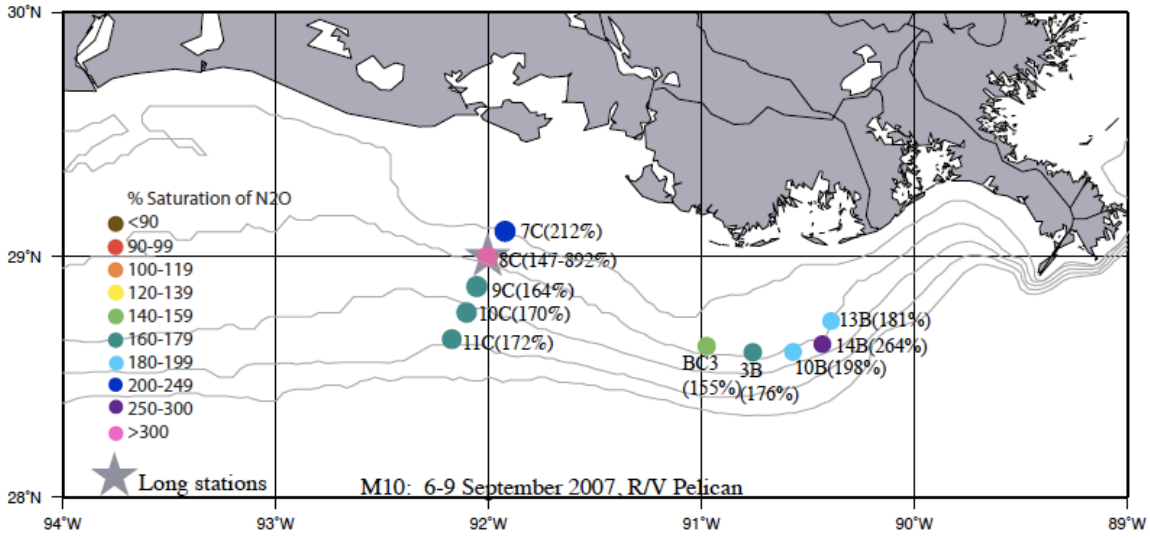

Figure 17. N_2O surface saturations (%) for the M10 (September 2007).

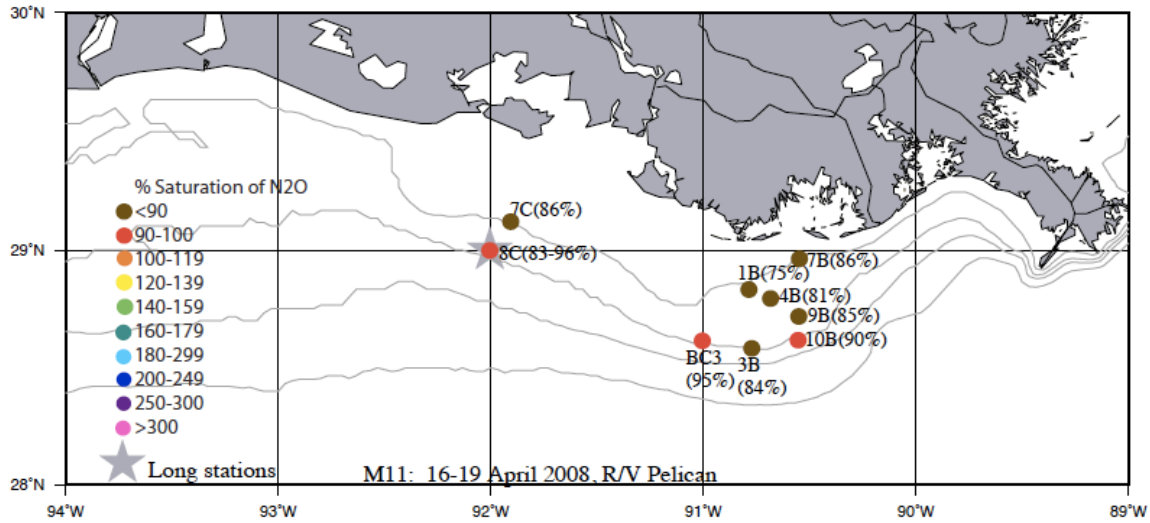

Figure 18. N_2O surface saturations (%) for the M11 (April 2008).

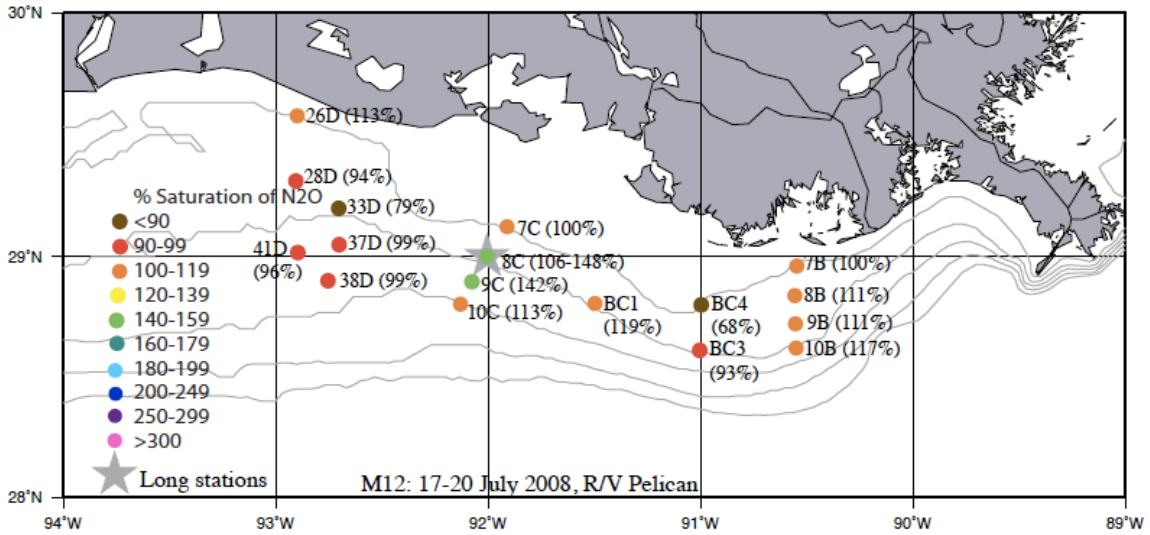

Figure 19. N_2O surface saturations (%) for the M12 (July 2008).

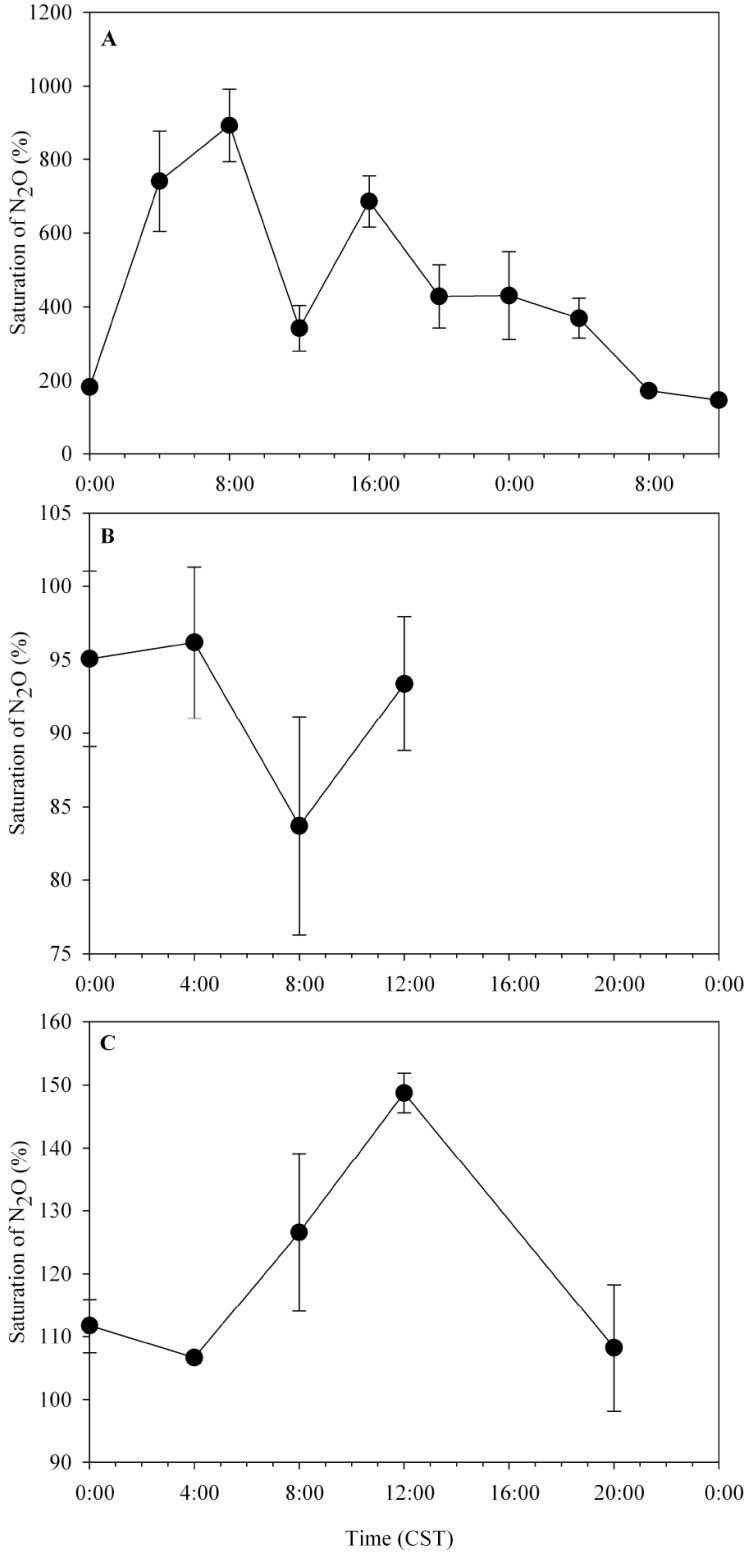

Figure 20. N_2O surface saturations (%) over time at station 8C for (A) M10 (September 2007), (B) M11 (April 2008), and (C) M12 (July 2008). Bars represent mean ± S.D.

4. DISCUSSION AND SUMMARY

4.1 Discussion of Hypotheses

The central hypothesis for this research was that *coastal hypoxic zones are significant sites for N_2O production due to the low oxygen and high inorganic nitrogen concentrations in the water column.* This hypothesis is accepted as N_2O concentrations reached 182.74 μmol m^{-3}, and the associated saturation was 2878 %. Water column oxygen concentrations were as low as 0.09 ml l^{-1}, and DIN reached 65.20 μmol l^{-1}.

The hypothesis that *The Gulf of Mexico hypoxic zone is a source of N_2O to the atmosphere* is also accepted as N_2O fluxes reached 153.22 μmol m^{-2} d^{-1}. The months of September (2007) and July (2008) were net sources of N_2O to the atmosphere, but the month of April (2008) was a sink.

The hypothesis that *there will be distinct seasonal changes in N_2O production associated with seasonal hypoxia* is accepted. The three cruises were significantly different from one another with respect to N_2O, and when hypoxia was present, N_2O concentration was greater.

It is unclear whether *Water column N_2O concentrations are higher at night than during the day.* Phytoplankton photosynthesis increases oxygen concentrations during the day, which may suppress pathways for N_2O production. However, diurnal changes in N_2O can be attributed to other physical and biological forces influencing hypoxia and N_2O production.

Sediment in the hypoxic zone is a source of N_2O to the overlying water column. This hypothesis is not accepted as sediment fluxes were low (-7.30 to 0.08 μmol m^{-2} d^{-1}) which suggests that the sediment is not a significant source of N_2O to the water column.

4.2 Water Column Processes

The Gulf of Mexico hypoxic zone is a significant site for N_2O production. The observed N_2O accumulation in the water column was due to low DO, high inorganic nitrogen and strong water stratification. Remineralization of organic matter occurred at the base of the pycnocline and oxycline producing high concentrations (up to 182.74 μmol m^{-3}) of N_2O in the water column (generally around 10m). During the summer when stratification was the strongest, depths were significantly different from one another with respect to N_2O concentration. A strong seasonal pycnocline and oxycline corresponding to a large spike in N_2O strongly resembles the characteristics of Oxygen Minnimum Zones (OMZs). Castro-Gonzalez & Farias (2004) found that in the OMZ off Northern Chile, denitrifiers are able to produce more N_2O from NO_2^- reduction when oxygen concentration increases to 22.3 µM (0.50 ml l^{-1}). Further lab results showed enhanced N_2O production for oxygen levels between 22 and 111 µM (0.49 and 2.48 ml l^{-1}) (Castro-Gonzalez and Farias 2004). Oxygen, along with electron donor and acceptor availability, is a key factor in regulating N_2O cycling. The low correlation coefficient between N_2O and oxygen, and the peaks of N_2O at the oxycline found in this study may indicate a non-linear response in N_2O production to oxygen concentrations. This response is not uncommon in estuarine waters and dynamic coastal systems, which illustrates the importance of these areas as sources of N_2O (De Bie et al. 2002). These

rates should be investigated further with the use of inhibitors, i.e. acetylene, and nutrient additions to determine the activity of enzymes present. Acetylene inhibits the enzyme nitrous oxide reductase, so N_2O accumulation can be measured in response to factors such as oxygen concentration or nutrient availability (Firestone & Teidje 1979).

The positive correlation of N_2O with both temperature and salinity and negative correlation with oxygen concentration is characteristic of denitrifying environments. However, the correlation coefficients were low which indicates that other factors, such as quality and source of organic matter may be important, or there may be interactions between multiple factors. The application of multivariate statistical techniques could be used to explore the relationships between the factors affecting N_2O production. Nutrient concentrations alone do not necessarily give an indication of the processes responsible for N_2O production. For example, low nitrite concentrations may indicate occurrence of denitrification to N_2O or N_2, or nitrification to nitrate. On the other hand, high nitrite concentrations may also indicate the potential for denitrification. During N_2O formation, the amount of standard free energy produced (from a mole of H_2) is greater using nitrite (ΔG = -226.5 KJ mol of H_2^{-1}) as an electron acceptor than nitrate (ΔG = -198.4 KJ mol H_2^{-1}) (Dong et al 2002). Because nitrite is a more energetically advantageous electron acceptor, low nitrite high nitrate conditions could indicate denitrification is the primary process responsible for N_2O production in energy limiting environments. However, there is a large supply of organic matter and nutrients to the pycnocline, so coupled nitrification-denitrification is more likely to occur at the pycnocline, and denitrification under limited resources is more likely to occur in the sediments (see 4.5)

The highest water column concentrations reported in the study area (183 μmol m^{-3}) are similar to those reported by Codispoti et al. (1992) in the coastal waters off Peru (173 μmol m^{-3}), but were not as great as those reported by Naqvi et al. (2000) in the low oxygen zone off the western India shelf (533 μmol m^{-3}). However, the western India shelf hypoxia covers a much greater area (180,000 km^2) than the Gulf of Mexico hypoxic zone, and it is influenced by moderate upwelling, which delivers nutrients to the sub-pycnocline. The Gulf of Mexico hypoxic zone is nutrient enriched from the Mississippi and Atchafalaya river plume, with nutrients delivered to the waters above the pycnocline. There were, however, similarities between these two systems in that most of the N_2O accumulation was subsurface, they were both reducing environments, hypoxia is seasonally dependent, and they are both a source of N_2O to the atmosphere. Flux rates for these areas were comparable, as the western India shelf rates were 40 to 268 μmol m^{-2} d^{-1}, compared with -11.27 to 153.22 μmol m^{-2} d^{-1} for the Texas-Louisiana shelf.

Bottom N_2O concentrations were lower than expected likely due to either reduction of N_2O with decreasing DIN resulting in N_2 as the final product of denitrification, or inhibition of nitrification from decreasing oxygen concentrations, resulting in less NO_3^- production available for denitrification.

N_2O production associated with hypoxia exhibited distinct seasonal changes. Spring river outflow created nutrient-enhanced primary productivity, hypoxia, and enhanced N_2O production in the summer. In April, hypoxia was virtually absent and N_2O production low likely because the water column was well mixed and because the spring river outflow had not made it to the shelf yet. Hypoxia and N_2O production dissipated at the end of the summer and variability in N_2O production in September may be due to

benthic respiration rather than river plume dependent water column respiration (Hetland & DiMarco 2008).

4.3 N_2O Emissions

Seasonal hypoxia in the Northern Gulf of Mexico creates a source of N_2O to the atmosphere. Surface saturations reached 2878 % and flux rates were as high as 153 μmol m^{-2} d^{-1}. Gas transfer velocities measured over longer time periods with variable winds are generally higher than those measured with instantaneous wind speeds, (Wanninkhof 1992) so calculated flux rates may be an underestimation. Also, values might be an underestimation due to the sub-surface transport of N_2O in the water column and subsequent ventilation into the atmosphere elsewhere. However, because of the temperature constraints of the Schmidt number calculations (0 to 30°C), where sea surface temperatures exceed 30°C, flux values are a slight over-estimation. The model was still used however, because temperatures did not exceed 31.8 °C, and the resulting increase in flux from 1.8 ºC was just 2 μmol m^{-2} d^{-1} from the current model.

Net efflux for each month was calculated from surface N_2O concentrations and extrapolated to an 20,000 km^2 area of hypoxia. This area was chosen because the maximum size of hypoxia in 2008 was 20,720 km^2 and in 2007 it was 20,460 km^2 (NOAA news 1 August 2007). For the month of September (2007) flux rates yielded a source of 2.66 x 10^{-3} Tg N_2O. July (2008) for this area yielded a source of 4.02 x 10^{-4} Tg N_2O. However, in April (2008) the 20,000 km^2 area where hypoxia would occur exhibited a sink for N_2O of -1.50 x 10^{-4} Tg N_2O. Considering hypoxia lasts 3 to 5 months, the area of seasonal hypoxia may create a source of N_2O to the atmosphere that

is not counterbalanced by a 7 to 9 month sink period. On the Indian shelf, Naqvi et al (2000) found a net efflux of 0.06 ± 0.39Tg of N_2O over a period of six months and an area 9 times greater than the Gulf of Mexico hypoxic zone. The annual flux of N_2O in the Arabian sea was calculated to be 0.2 to 2 Tg N_2O $year^{-1}$ (using a general circulation model consisting of 13 depth layers rather than surface calculations) (Bange 2000).

4.4 Storage and Air Sample Considerations

The variability in the M10 (September 2007) samples may be due to longer strorage time before the samples were analyzed; the M10 (September 2007) and M10 (September 2007) samples were analyzed within one month while some of the M10 (September 2007) samples were analyzed after several months because of instrument maintenance. Although the storage experiment indicated the change in N_2O over time may only be due to random sampling variability, after 6 months the vials appear to begin equilibration with the air. This should not have an effect on the cruise samples however, because they were generally analyzed within 1 month, the range of N_2O in the cruise samples was much larger, and changes in N_2O in the water column are clearly visible. The lowest N_2O concentration recorded from the cruises (4.72 μmol m^{-3}) was higher than the "low" samples from the strorage experiment, indicating either some atmospheric N_2O entered the cruise sample, or the "low" storage experiment sample was not a good representation of the field conditions. After several months of storage, low concentrations were still seen in the cruise samples. Ideally, the GC should have been placed onboard the ship to enable immediate analysis of the samples and thereby avoid potential changes in the samples caused by storage. However, logistically this was not

feasible. Firstly, the cruises were of such short duration that there was not sufficient time to set up and allow the GC to stabilize prior to arriving at the first station. Secondly, this approach would have required more ship-board personnel and space, which were not available.

Air samples taken during the cruise were variable and usable samples ranged from 310 to 424 ppbv. However, most air samples were not usable so the measured concentrations were not used in any calculations. Contamination issues occurred in the air samples from inability to escape ship exhaust during collection, and from a different type of vial that was used to collect some samples. The air samples taken in the same Agilent vials that were used for water collection did not have contamination, but Vacutainers were also used to collect air, and the stoppers leached unknown compounds into the sample. As a result of this, the global average mixing ratio of 319 ppbv N_2O (IPCC 2007) was used for all saturation and flux calculations.

4.5 Benthic Fluxes

The sediments exhibit high variability in sources and sinks for N_2O, and the processes producing and consuming N_2O are unclear. In order to determine *in situ* flux rates for the hypoxic zone, a shorter incubation time would be necessary and a higher number of samples for precision. Over long incubation times, N_2O may initially be produced via denitrification, but as the NO_3^- and NO_2^- in the closed core system are used up, N_2O then becomes reduced to N_2.

DNRA, the anaerobic pathway favored by microbes in the presence of H_2S (Childs et al. 2002) is another likely pathway to produce N_2O in sediments. However, no

sulfate reduction or H_2S accumulation was found at 4 representative stations in the hypoxic zone in April (2008) or July (2008) (Brandi Kiel Reese pers. Comm.) indicating DNRA might not be a primary pathway for N_2O production. However, these sites were west of the Mississippi and Atchafalaya river mouths and thus farther from the source of organic matter. Also, sediments that remain hypoxic throughout the summer may be limited in the availability of organic substrates and oxidizing agents, which creates competition for resources. In this scenario, denitrification of nitrate to form N_2 is most energetically favorable (ΔG = -1,120.5 KJ mol H_2^{-1}) followed by reduction of N_2O to N_2 (ΔG = -341.1 KJ mol H_2^{-1}) (Dong et al 2002). Sediments closer to the river mouths are rich in labile organic matter and more favorable for N_2O production. During hypoxia *in situ*, N_2O may be the final product of denitrification when there is potentially a continuous nutrient supply to the sediment, such as in the sediment closer to the mouth of the rivers.

4.6 Future Considerations

With increasing atmospheric CO_2 concentrations (lowering the ratio of pO_2 to pCO_2) and rising ocean temperatures depleting bottom oxygen concentrations, oceanic dead zones may be widely expanding (Brewer 2009). A decreasing ratio of pO_2 to pCO_2 will inhibit aerobic respiration and increase N_2O at depth (Brewer 2009). For higher animals, "dead zones" may be redefined to oxygen levels where normal respiration is inhibited, and these dead zones for aerobic life are likely to grow in size (Brewer 2009). The effect of climate change on the well-oxygenated open ocean will be much different than in the Gulf of Mexico Hypoxic zone. Anthopogenic activity increases N supply to

the coastal ocean, decreasing O_2 availability and increasing N_2O emissions (Naqvi et al. 2000; Nevison et al. 2004). The addition of N into coastal waters from rivers is not the only factor to consider; anthropogenic atmosperic deposition of fixed nitrogen, N_r (NO_x or $NO + NO_2$) has resulted in the production of up to 1.6 Tg N_2O-N $year^{-1}$ (Duce et al. 2008). However, primary production as a result of anthropogenic atmospheric nitrogen (up to ~ 0.3 pg C $year^{-1}$) removes CO_2 from the atmosphere and decreases radiative forcing casued by N_r (Duce et al. 2008). Duce et al. (2008) suggest the increase N_2O emissions offsets two-thirds of the decrease in radiative forcing from the decrease in CO_2. These results show that climate change and anthopogenic activity will enhance seasonal hypoxia, and without efforts to counteract this scenario, the associated N_2O flux is likely to increase.

A reduction of nitrogen loading to the Texas-Louisiana shelf is not only necessary to reduce hypoxia, but also to reduce the amount of N_2O produced in this area. Further research on the processes responsible for N_2O production, i.e. enzymatic activity and relative contribution of nitrification and denitrification, could facilitate development of a model that uses Mississippi and Atchafalaya river DIN export rates, along with other physical factors, to estimate emission of N_2O. The current global model (Seitzinger and Kroeze 1998) does not take into account N_2O production in the Gulf of Mexico. A higher spatial and temporal resolution of N_2O in the surface waters would be necessary to determine the magnitude of the annual N_2O efflux. This study shows that N_2O should be taken into consideration when discussing the environmental impacts of Gulf of Mexico hypoxia. Quantifying the sources and sinks of N_2O in the Gulf of Mexico hypoxic zone

enhances our overall understanding of coastal hypoxic areas, as these areas may contribute a significant portion of global N_2O production.

LITERATURE CITED

Armstrong FA, Stearns CR, Strickland, JD (1967) The measurement of upwelling and subsequent biological processes by means of the Technicon Autoanalyzer and associated equipment. Deep-Sea Research Part A-Oceanographic Research Papers 14(3)381-389

Bange HW (2000) Global change - It's not a gas. Nature 408:301-302

Bange HW, Andreae MO, Lal S, Law CS, Naqvi SWA, Patra PK, Rixen T, Upstill-Goddard RC (2001) Nitrous oxide emissions from the Arabian Sea: A synthesis. Atmospheric Chemistry and Physics 1:61-71

Bange HW, Rapsomanikis S, Andreae MO (1996) Nitrous oxide emissions from the Arabian Sea. Geophysical Research Letters 23:3175-3178

Bernhardt H, Wilhelms A (1967) The continuous determination of low level iron, soluble phosphate and total phosphate with the AutoAnalyzer. Technicon Symposium

Bonin P, Tamburini C, Michotey V (2002) Determination of the bacterial processes which are sources of nitrous oxide production in marine samples. Water Research 36:722-732

Bouwman AF, Vanderhoek KW, Olivier JGJ (1995) Uncertainties in the global source distribution of nitrous oxide. Journal of Geophysical Research-Atmospheres 100:2785-2800

Butler JH, Elkins JW, Thompson TM, Egan KB (1989) Tropospheric and dissolved N_2O of the West Pacific and East Indian Oceans during the El-Nino southern

oscillation event of 1987. Journal of Geophysical Research-Atmospheres 94:14865-14877

Castro-Gonzalez M, Farias L (2004) N_2O cycling at the core of the oxygen minimum zone off northern Chile. Marine Ecology Progress Series 280:1-11

Committee on Environment and Natural Resources (CENR) (2000) National Assessment of Harmful Algal Blooms in U.S. Waters. National Science and Technology Council, Washington, D.C.

Childs CR, Rabalais NN, Turner RE, Proctor LM (2002) Sediment denitrification in the Gulf of Mexico zone of hypoxia. Marine Ecology-Progress Series 240:285-290

Codispoti LA, Elkins JW, Yoshinar T, Friederich GE, Sakamoto LM, Packard TT (1992) On the nitrous oxide flux from productive regions that contain low oxygen waters. IN: Desai BN (ed) Oceanography of the Indian Ocean. Oxford and IBH, New Delhi, p 271-284

De Bie MJM, Middelburg JJ, Starink M, Laanbroek HJ (2002) Factors controlling nitrous oxide at the microbial community and estuarine scale. Marine Ecology-Progress Series 240:1-9

Duce RA, LaRoche J, Altieri K, Arrigo KR, Baker AR, et al. (2008) Impacts of atmospheric anthropogenic nitrogen on the open ocean. Science 320:893-897

Diaz RJ, Rosenberg R (2008) Spreading dead zones and consequences for marine ecosystems. Science 5891(321):926-929

DiMarco, SF (March 2009) Personal Communication

Dong LF, Nedwell DB, Underwood GJC, Thornton DCO, Rusmana I (2002) Nitrous oxide formation in the Colne estuary, England: The central role of nitrite. Applied and Environmental Microbiology 68:1240-1249

Dong LF, Nedwell DB, Stott A (2006) Sources of nitrogen used for denitrification and nitrous oxide formation in sediments of the hypernutrified Colne, the nutrified Humber, and the oligotrophic Conwy estuaries, United Kingdom. Limnology and Oceanography 51:545-557

EPA (2007) Hypoxia in the Northern Gulf of Mexico: an update by the EPA science advisory board. Report No. EPA-SAB-08-003, Washington, DC

Erickson DJ (1993) A stability dependent theory for air-sea gas exchange. Journal of Geophysical Research 98:8471-8488

Firestone MK, Tiedje JM (1979) Temporal change in nitrous oxide and dinitrogen from denitrification following onset of anaerobiosis. Applied Environmental Microbiology 38(4):673-679

Gardner WS, Briones EE, Kaegi EC, Rowe GT (1993) Ammonium excretion by benthic invertebrates and sediment-water nitrogen flux in the Gulf of Mexico near the Mississippi river outflow. Estuaries 16:799-808

Harwood JE, Kuhn A, Kerovel R (1970) A colorimetric method for ammonia in natural waters. Water Research 4:805-811

Hetland RD, DiMarco SF (2008) How does the character of oxygen demand control the structure of hypoxia on the Texas-Louisiana continental shelf? Journal of Marine Systems 70(1-2):49-62

IPCC (2001) Climate Change 2001: Synthesis Report. A Contribution of Working Groups I, II, and III to the Third Assessment Report of the Intergovernmental Panel on Climate Change. Cambridge Univ. Press, Cambridge, UK

IPCC (2007) Climate Change 2007: The Physical Science Basis. Contribution of Working Group I to the Fourth Assessment Report of the Intergovernmental Panel on Climate Change. Cambridge Univ. Press, Cambridge, UK

Jorgensen KS, Jensen HB, Sorensen J (1984) Nitrous oxide production from nitrification and denitrification in marine sediment at low oxygen concentrations. Canadian Journal of Microbiology 30:1073-1078

Khalil MAK, Rasmussen RA (1992) The global sources of nitrous oxide. Journal of Geophysical Research-Atmospheres 97:14651-14660

Khalil MAK, Rasmussen RA, Shearer MJ (2002) Atmospheric nitrous oxide: patterns of global change during recent decades and centuries. Chemosphere 47:807-821

Kirkwood D (1996) Nutrients: a practical note on their determination in seawater. Techniques in marine environmental science no. 17. ICES, Copenhagen, Denmark

Kroeze C, Dumont E, Seitzinger SP (2005) New estimates of global emissions of N_2O from rivers and estuaries. Environmental Science 2:159-165

LUMCON (28 July 2008) 'Dead Zone' Again Rivals Record Size. Press Release, Louisiana University Marine Consortium. http://www.lumcon.edu/Information/news/default.asp?XMLFilename=200807281352.xml.

Montzka SA, Fraser, PJ (2003) Chapter 1: Controlled substances and other source gases. Scientific Assessment of Ozone Depletion: 2002 World Meteorological Organization, Geneva 47:1.1-1.83

Naqvi SWA, Jayakumar DA, Narvekar PV, Naik H, Sarma V, D'Souza W, Joseph S, George MD (2000) Increased marine production of N_2O due to intensifying anoxia on the Indian continental shelf. Nature 408:346-349

Nevison CD, Lueker TJ, Weiss RF (2004) Quantifying the nitrous oxide source from coastal upwelling. Global Biogeochemical Cycles 18:1018

NOAA, Sapp A (1 August 2007) Survey cruise records third-largest "dead zone" since 1985 area size of New Jersey close to NOAA-LSU prediction. NOAA News, Louisiana University Marine Consortium. http://www.noaanews.noaa.gov/stories2007/s2901.htm

Osterman LE, Poore RZ, Swarzenski PW, Turner RE (2005) Reconstructing a 180-yr record of natural and anthropogenic induced hypoxia from the sediments of the Louisiana continental shelf. Geology 33:329-332

Punshon S, Moore RM (2004) Nitrous oxide production and consumption in a eutrophic coastal embayment. Marine Chemistry 91:37-51

Rabalais NN, Harper DE, Turner RE (2001) Responses of nekton and demersal and benthic fauna to decreasing oxygen concentrations. Coastal and Estuarine Sciences 58:115-128

Rabalais NN, Turner RE, Sen Gupta BK, Boesch DF, Chapman P, Murrell MC (2007) Hypoxia in the northern Gulf of Mexico: Does the science support the plan to reduce, mitigate, and control hypoxia? Estuaries and Coasts 30:753-772

Rasmussen RA, Krasnec J, Pierotti D (1976) N_2O Analysis in atmosphere via electron capture gas chromatography. Geophysical Research Letters 3:615-618

Rowe GT (2001) Seasonal hypoxia in the bottom water off the Mississippi River delta. Journal of Environmental Quality 30:281-290

Seitzinger SP, Kroeze C (1998) Global distribution of nitrous oxide production and N inputs in freshwater and coastal marine ecosystems. Global Biogeochemical Cycles 12:93-113

Senga Y, Mochida K, Fukumori R, Okamoto N, Seike Y (2006) N_2O accumulation in estuarine and coastal sediments: The influence of H_2S on dissimilatory nitrate reduction. Estuarine Coastal and Shelf Science 67:231-238

Sloth NP, Blackburn H, Hansen LS, Risgaardpetersen N, Lomstein BA (1995) Nitrogen cycling in sediments with different organic loading. Marine Ecology Progress Series 116:163-170

Sweeney C, Gloor E, Jacobson AR, Key R, McKinley G, Sarmiento JL, Wanninkhof, R (2007) Constraining global air-sea gas exchange for CO_2 with recent bomb 14C measurements. Global Biogeochemical Cycles 21:2015

Vaquer-Sunyer R, Duarte CM (2008) Thresholds of hypoxia for marine biodiversity. Proceedings of the National Academy of Science of the United States of America 105:15452-15457

Wanninkhof R (1992) Relationship between wind speed and gas exchange over the ocean. Journal of Geophysical Research 97:7373-7382

Weiss RF (1981) The temporal and spatial-distribution of tropospheric nitrous oxide. Journal of Geophysical Research-Oceans and Atmospheres 86:7185-7195

Weiss RF, Price BA (1980) Nitrous oxide solubility in water and seawater. Marine Chemistry 8:347-359

Zumft WG (1997) Cell biology and molecular basis of denitrification. Microbiology and Molecular Biology Reviews 61:533-616.

APPENDIX A

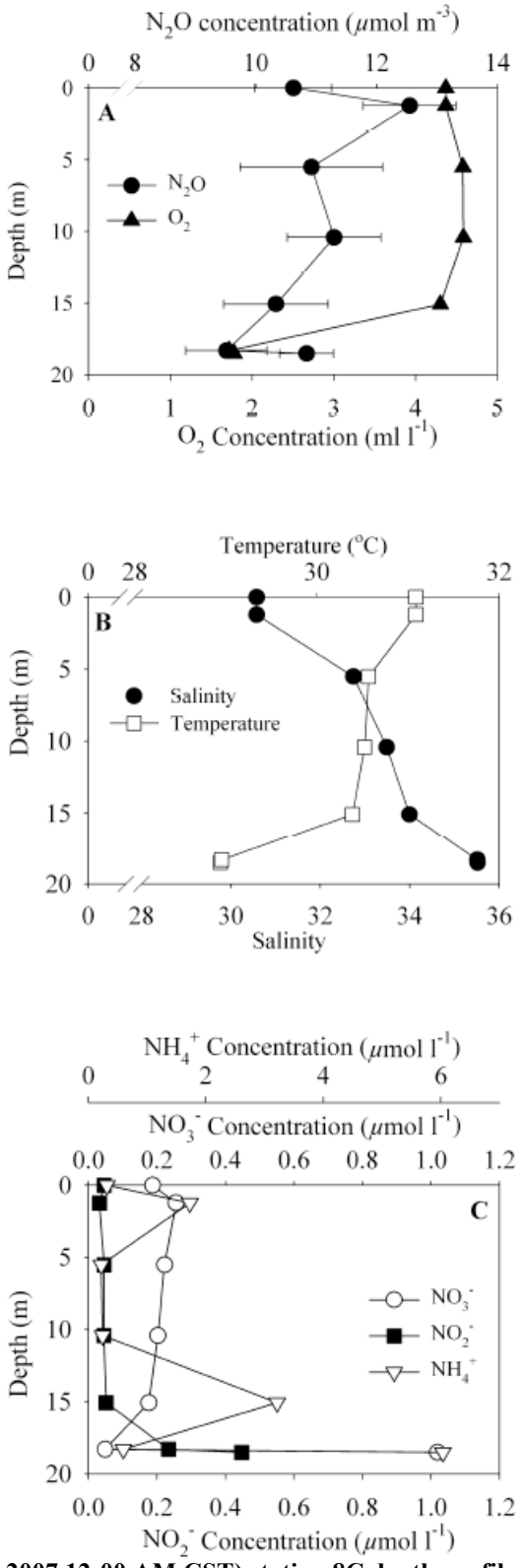

Figure A.1 M10 (September 2007 12:00 AM CST) station 8C depth profiles for (A) N_2O and O_2, (B) temperature and salinity, and (C) NH_4^+, NO_3^- and NO_2^-. Bars represent mean ± S.D.

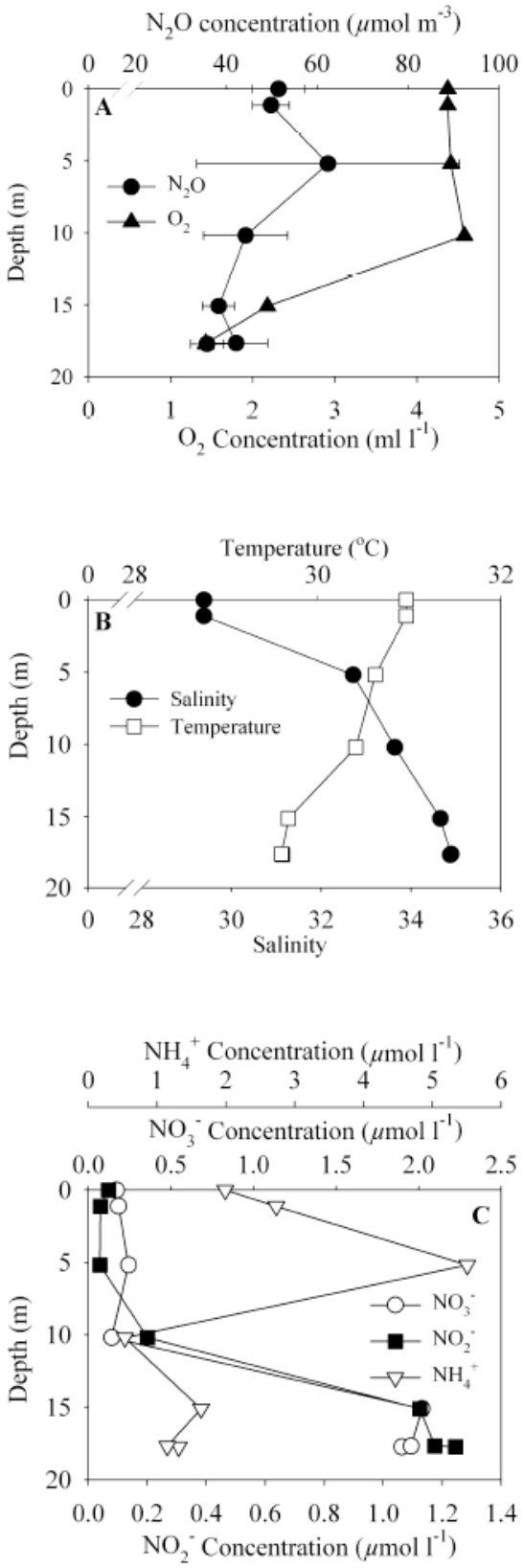

Figure A.2 M10 (September 2007 8:00 AM CST) station 8C depth profiles for (A) N_2O and O_2, (B) temperature and salinity, and (C) NH_4^+, NO_3^- and NO_2^-. Bars represent mean ± S.D.

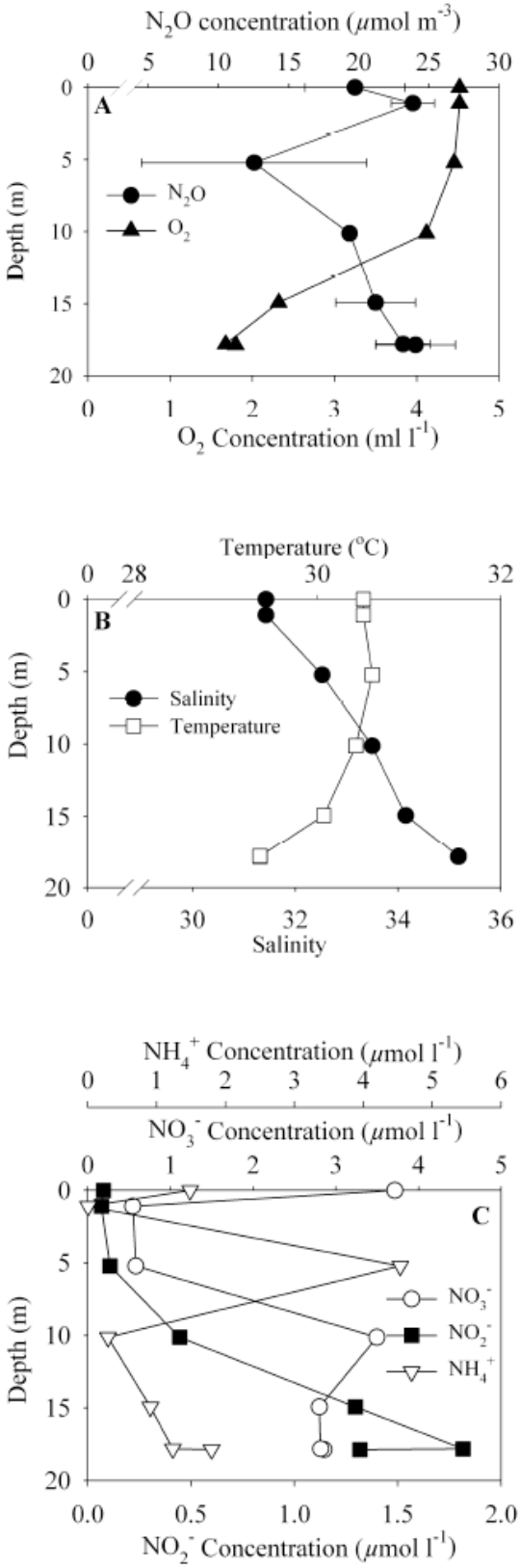

Figure A.3 M10 (September 2007 12:00 PM CST) station 8C depth profiles for (A) N_2O and O_2, (B) temperature and salinity, and (C) NH_4^+, NO_3^- and NO_2^-. Bars represent mean ± S.D.

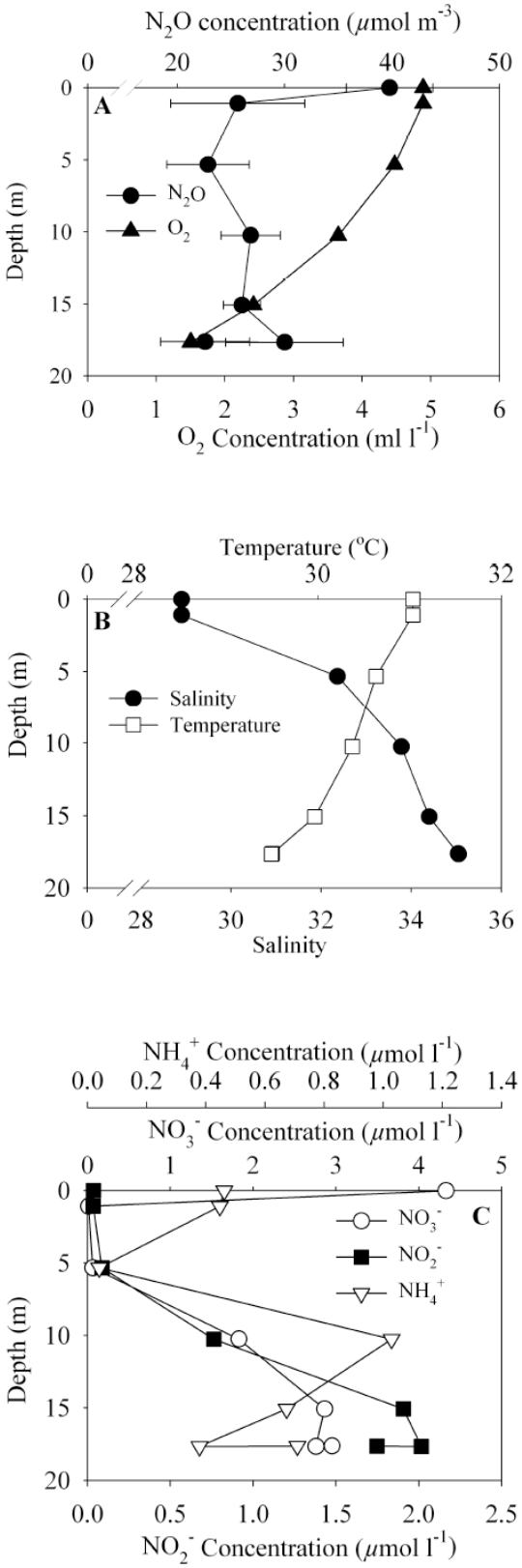

Figure A.4 M10 (September 2007 4:00 PM CST) station 8C depth profiles for (A) N_2O and O_2, (B) temperature and salinity, and (C) NH_4^+, NO_3^- and NO_2^-. Bars represent mean ± S.D.

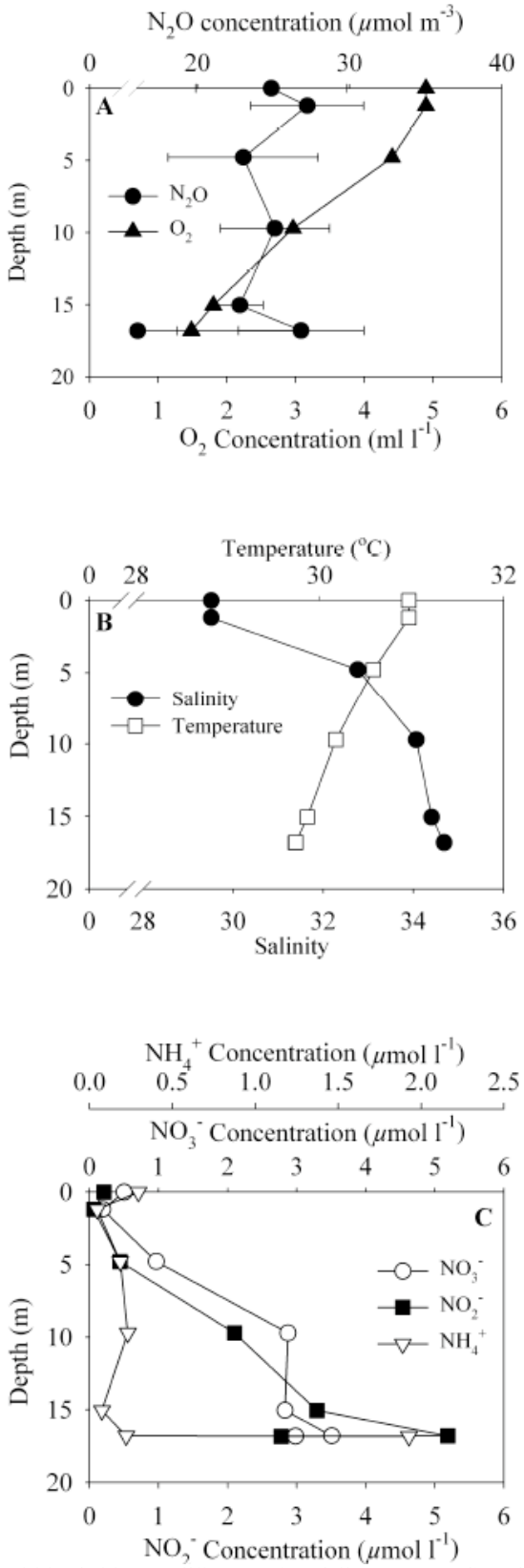

Figure A.5 M10 (September 2007 8:00 PM CST) station 8C depth profiles for (A) N_2O and O_2, (B) temperature and salinity, and (C) NH_4^+, NO_3^- and NO_2^-. Bars represent mean ± S.D.

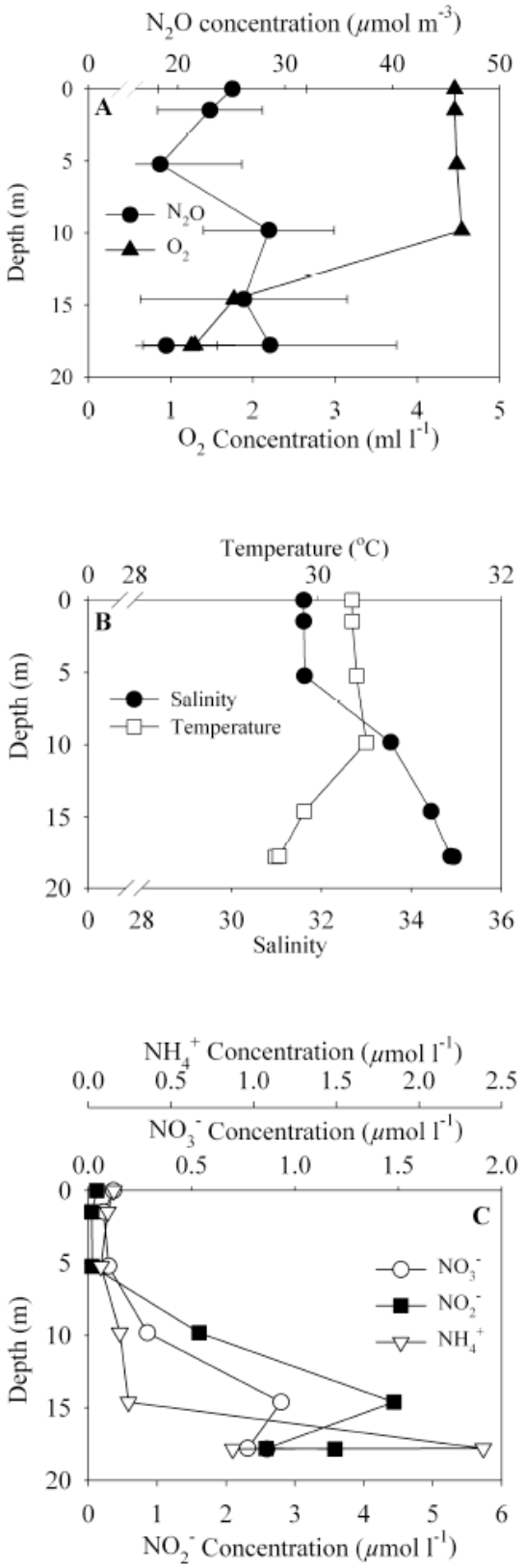

Figure A.6 M10 (September 2007 12:00 AM CST) station 8C depth profiles for (A) N_2O and O_2, (B) temperature and salinity, and (C) NH_4^+, NO_3^- and NO_2^-. Bars represent mean ± S.D.

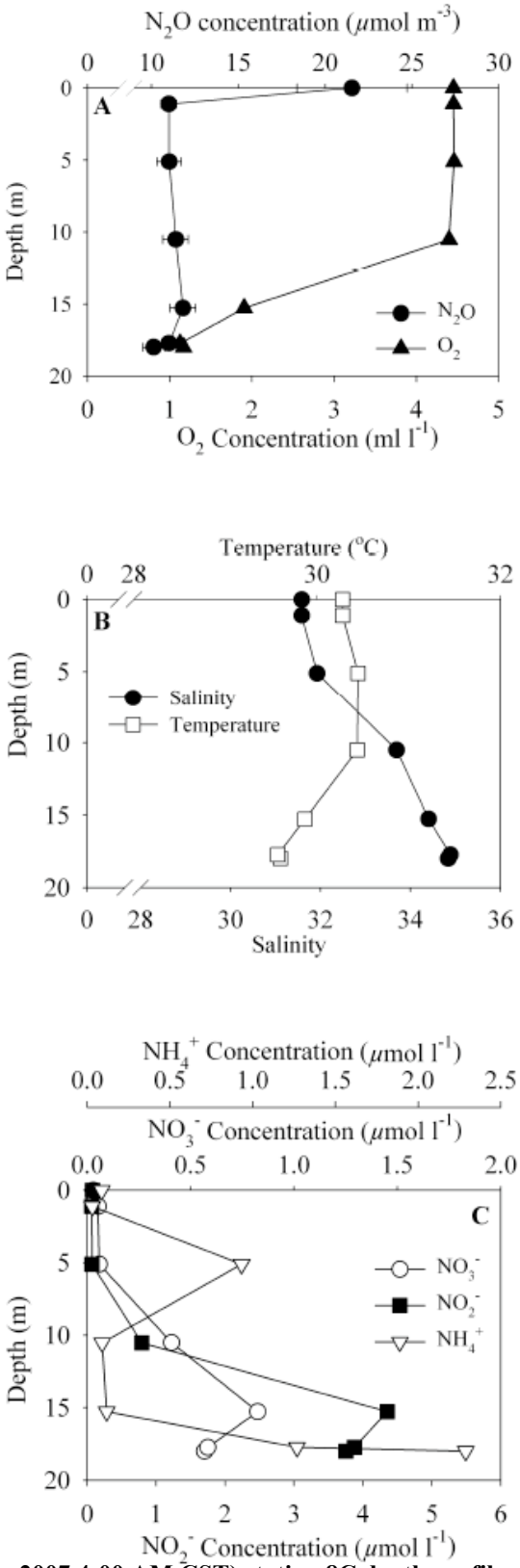

Figure A.7 M10 (September 2007 4:00 AM CST) station 8C depth profiles for (A) N_2O and O_2, (B) temperature and salinity, and (C) NH_4^+, NO_3^- and NO_2^-. Bars represent mean ± S.D.

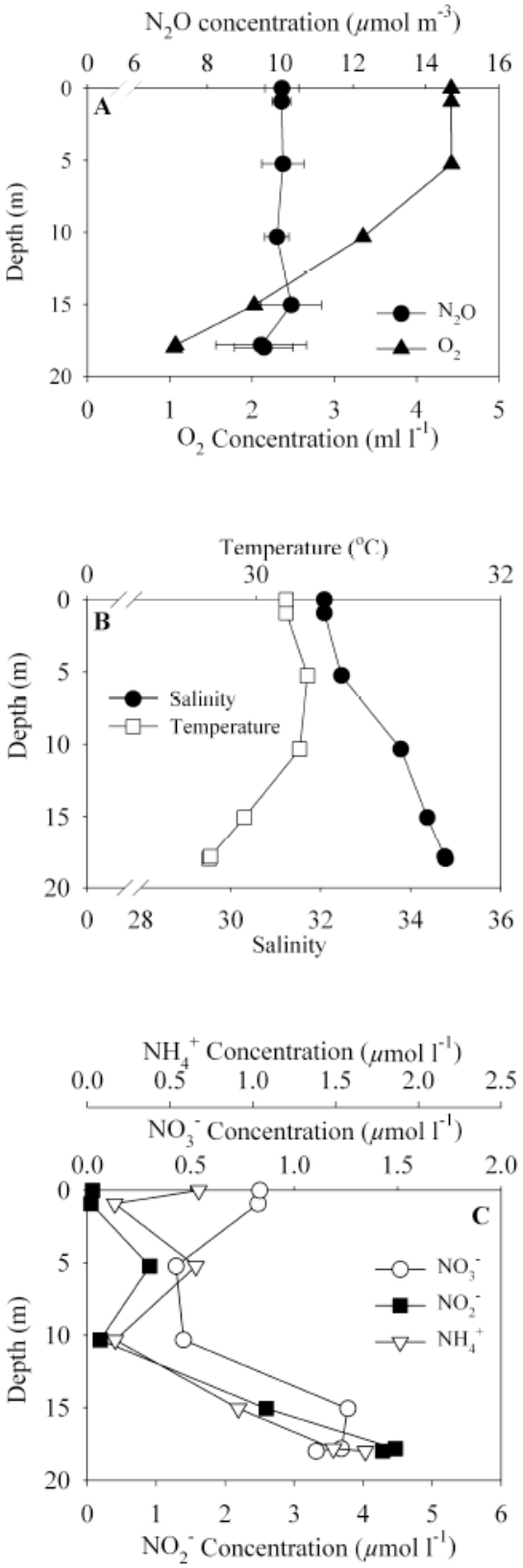

Figure A.8 M10 (September 2007 8:00 AM CST) station 8C depth profiles for (A) N_2O and O_2, (B) temperature and salinity, and (C) NH_4^+, NO_3^- and NO_2^-. Bars represent mean ± S.D.

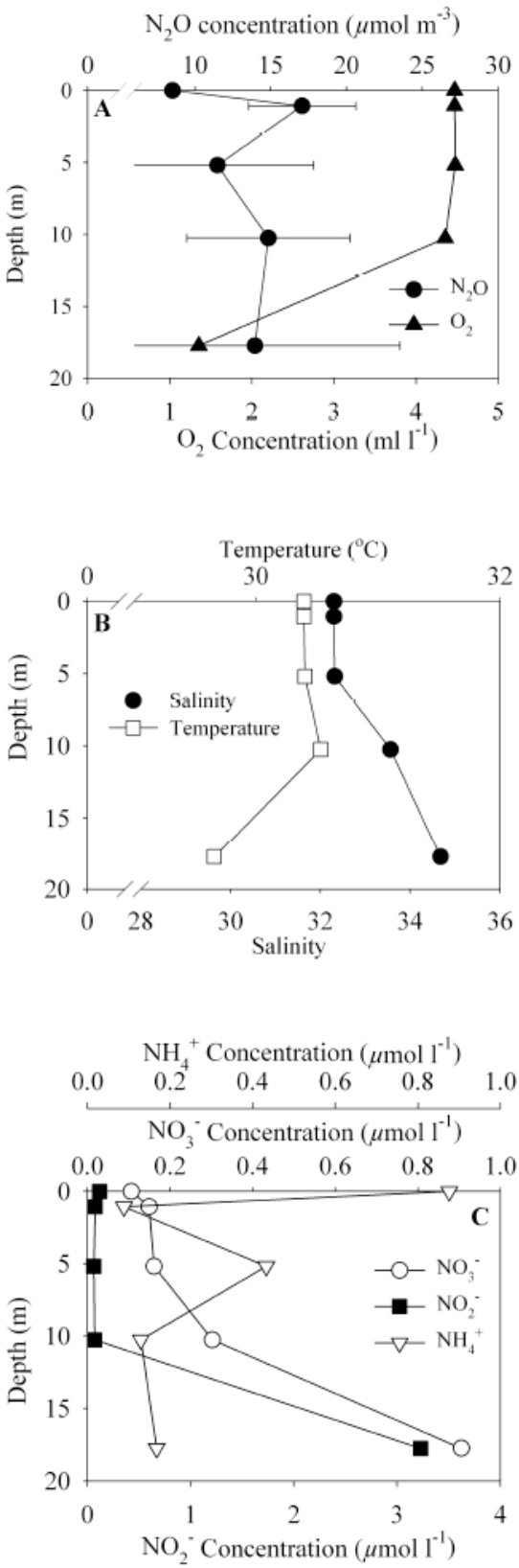

Figure A.9 M10 (September 2007 12:00 PM CST) station 8C depth profiles for (A) N_2O and O_2, (B) temperature and salinity, and (C) NH_4^+, NO_3^- and NO_2^-. Bars represent mean ± S.D.

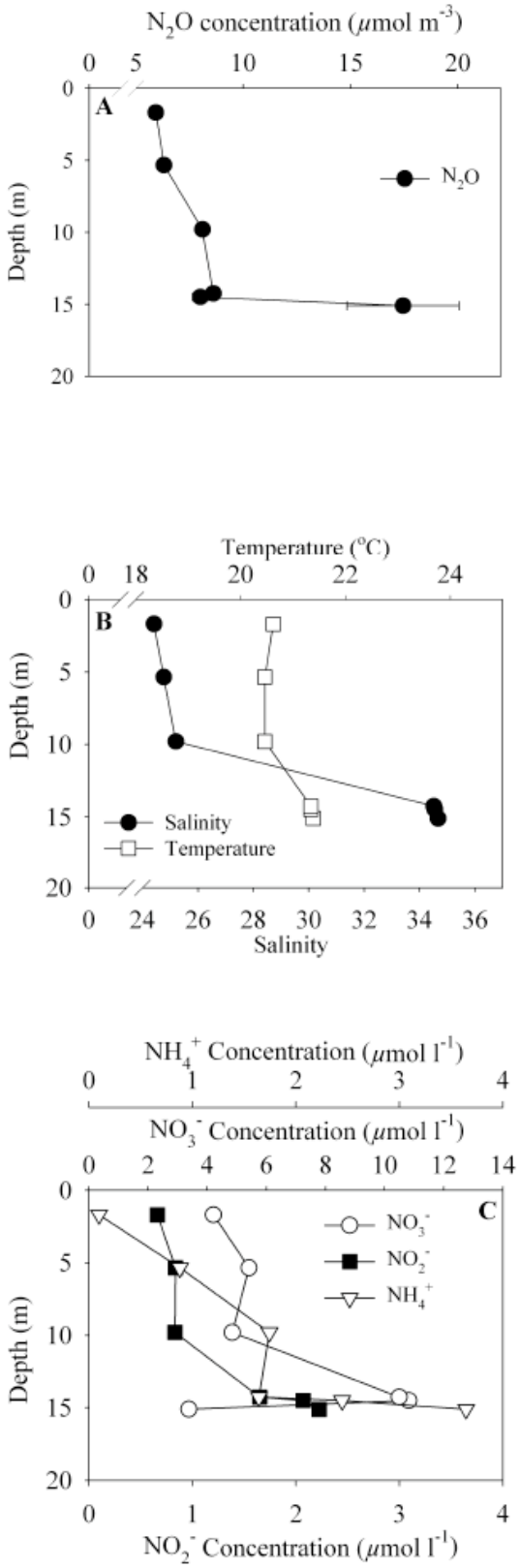

Figure A.10 M11 (April 2008) station 1B depth profiles for (A) N_2O, (B) temperature and salinity, and (C) NH_4^+, NO_3^- and NO_2^-. Bars represent mean ± S.D.

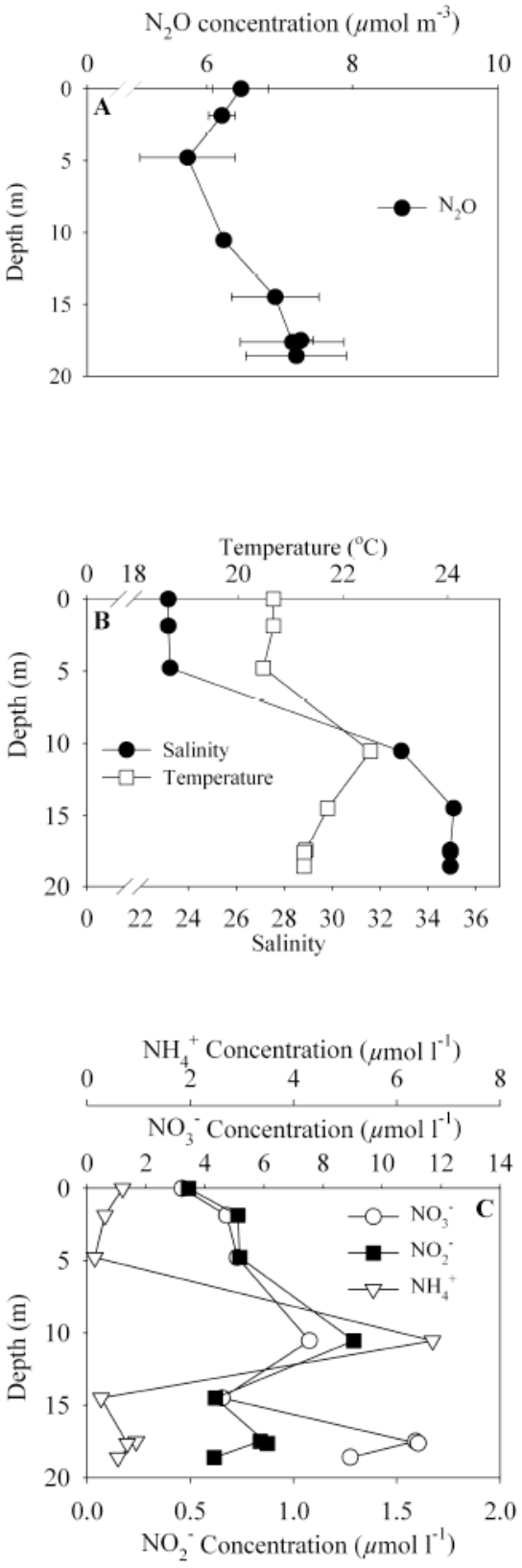

Figure A.11 M11 (April 2008) station 4B depth profiles for (A) N_2O, (B) temperature and salinity, and (C) NH_4^+, NO_3^- and NO_2^-. Bars represent mean ± S.D.

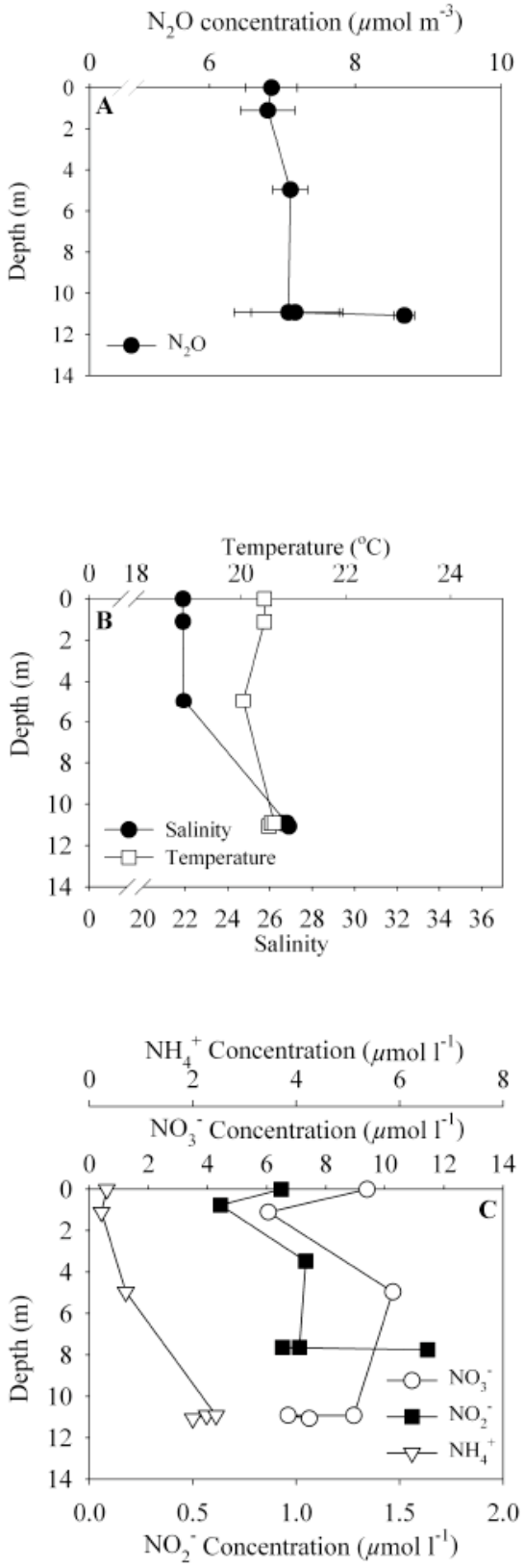

Figure A.12 M11 (April 2008) station 7B depth profiles for (A) N_2O, B) temperature and salinity, and (C) NH_4^+, NO_3^- and NO_2^-. Bars represent mean ± S.D.

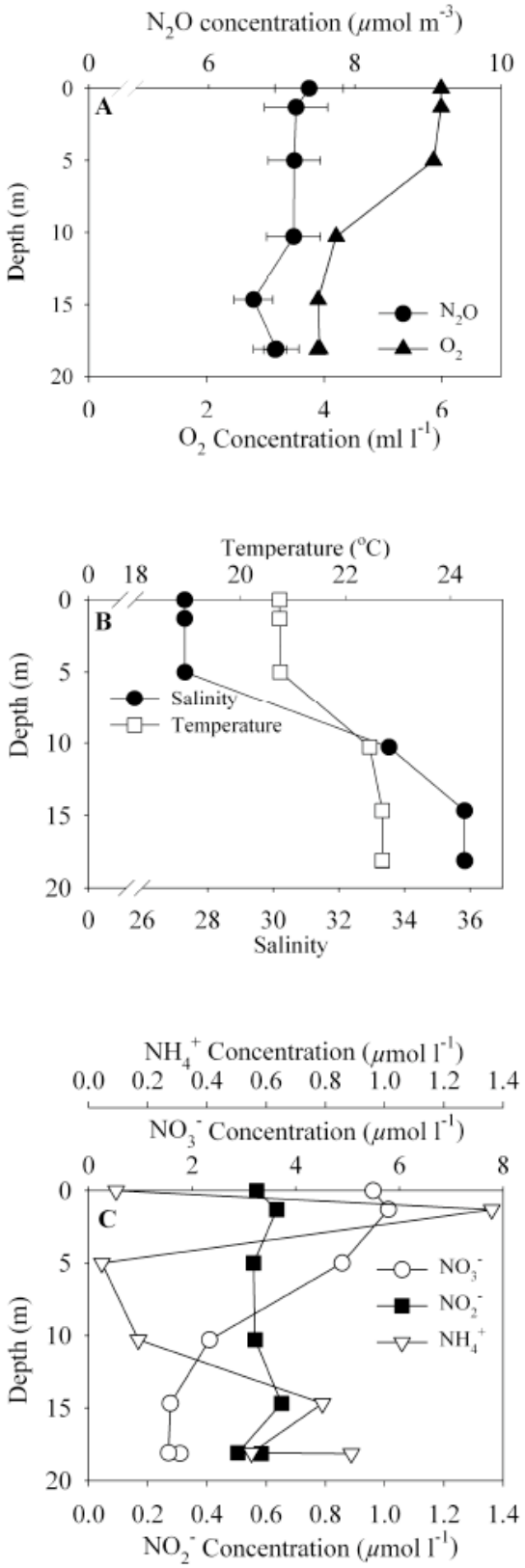

Figure A.13 M11 (April 2008 12:00 AM) station 8C depth profiles for (A) N_2O and O_2, (B) temperature and salinity, and (C) NH_4^+, NO_3^- and NO_2^-. Bars represent mean ± S.D.

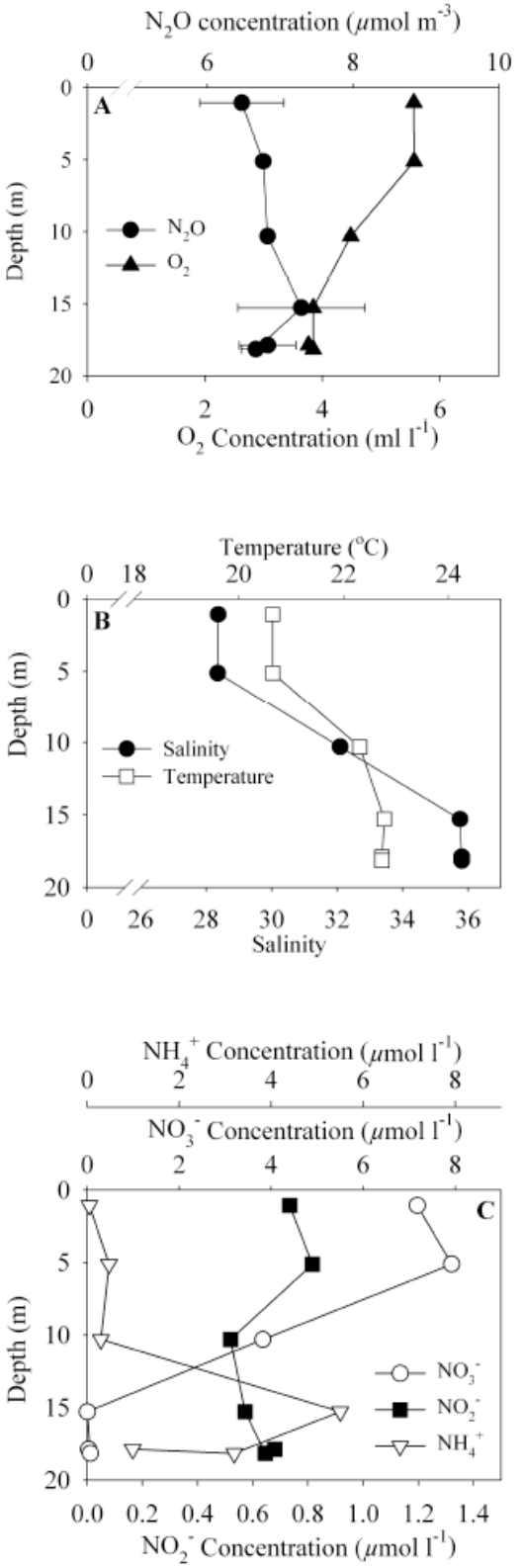

Figure A.14 M11 (April 2008 8:00 AM CST) station 8C depth profiles for (A) N_2O and O_2, (B) temperature and salinity, and (C) NH_4^+, NO_3^- and NO_2^-. Bars represent mean ± S.D.

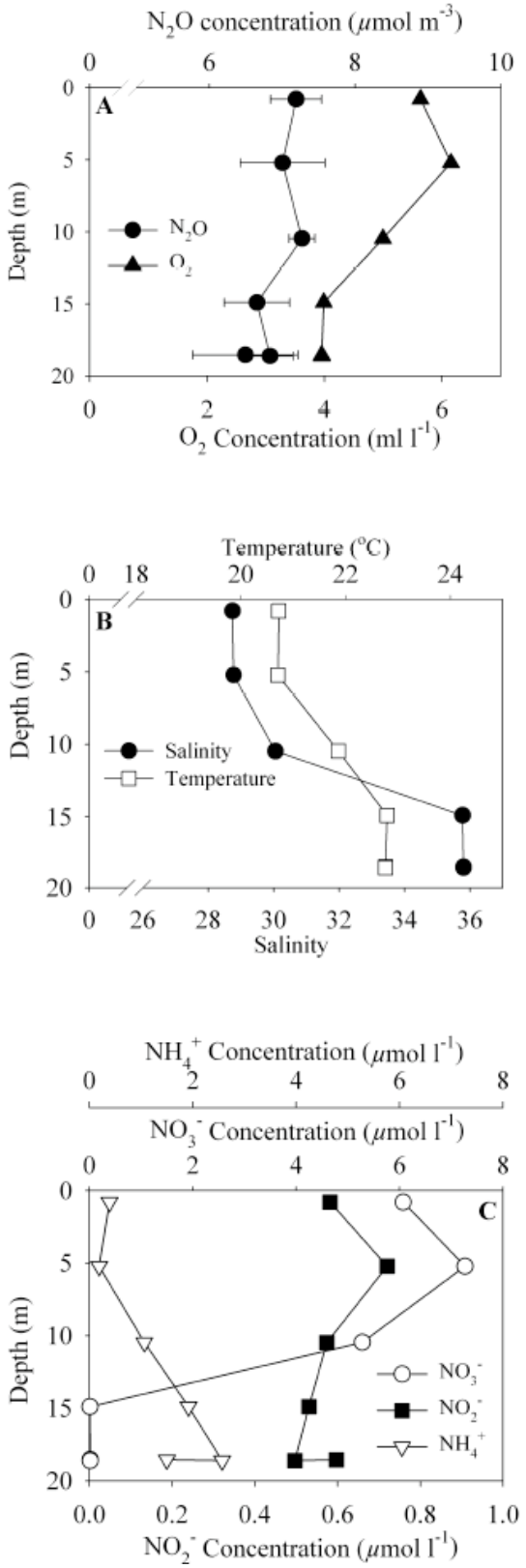

Figure A.15 M11 (April 2008 12:00 PM CST) station 8C depth profiles for (A) N_2O and O_2, (B) temperature and salinity, and (C) NH_4^+, NO_3^- and NO_2^-. Bars represent mean ± S.D.

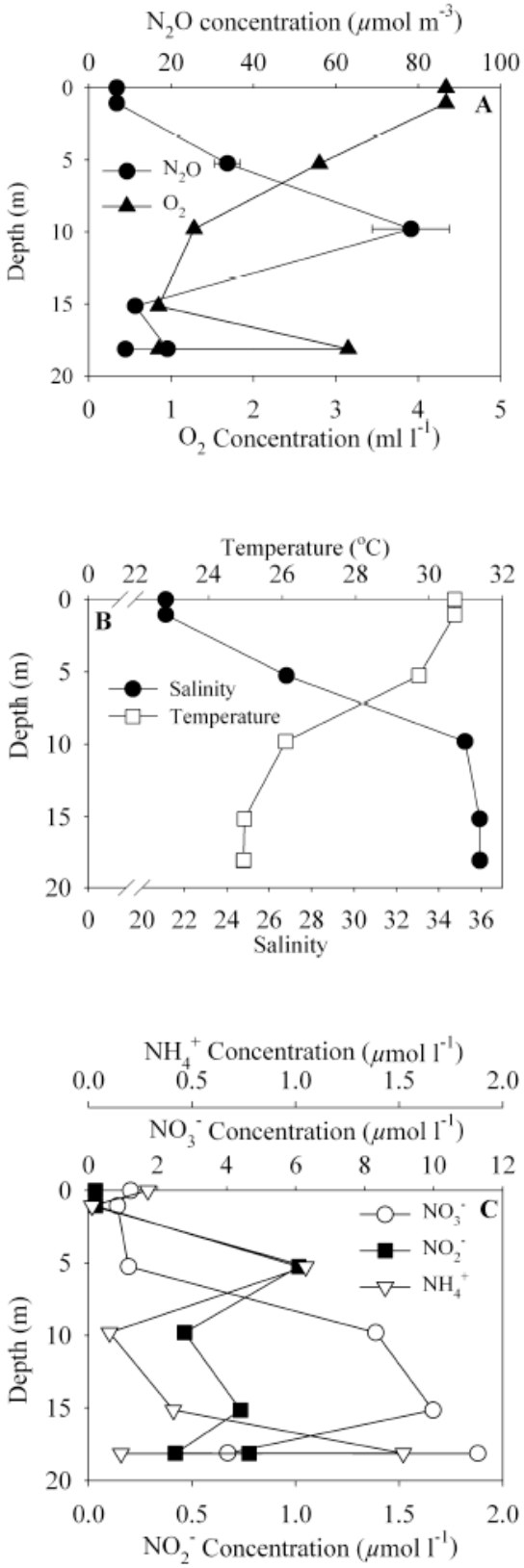

Figure A.16 M12 (July 2008 12:00 AM CST) station 8C depth profiles for (A) N_2O and O_2, (B) temperature and salinity, and (C) NH_4^+, NO_3^- and NO_2^-. Bars represent mean ± S.D.

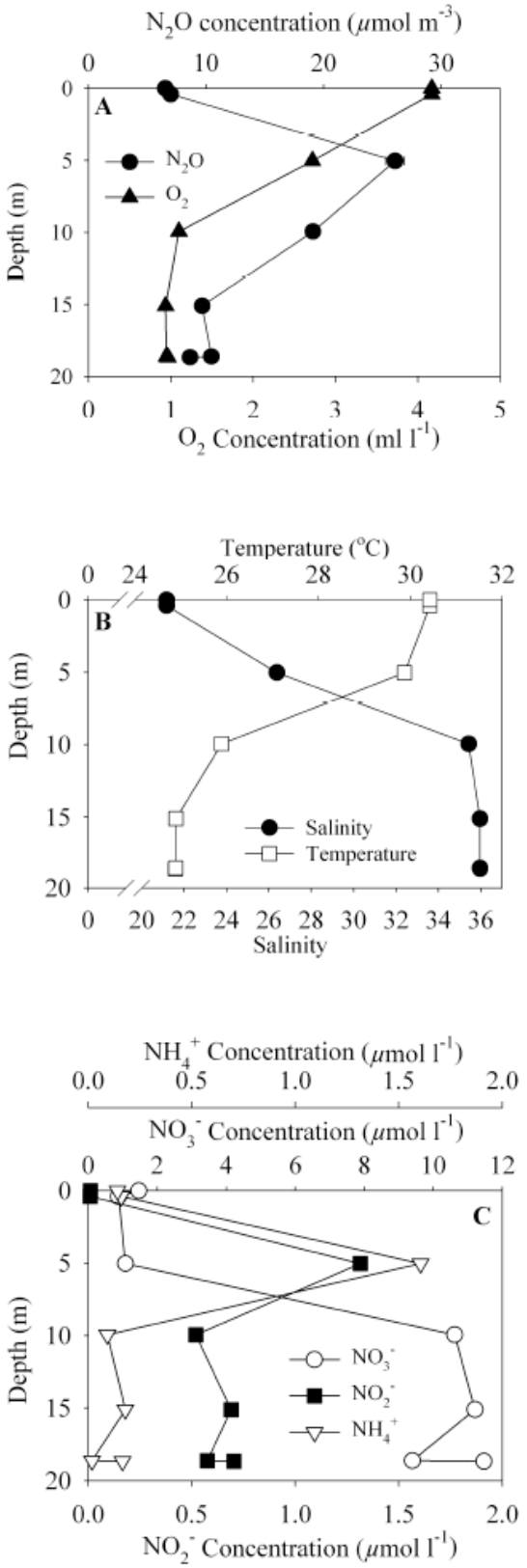

Figure A.17 M12 (July 2008 4:00 AM CST) station 8C depth profiles for (A) N_2O and O_2, (B) temperature and salinity, and (C) NH_4^+, NO_3^- and NO_2^-. Bars represent mean ± S.D.

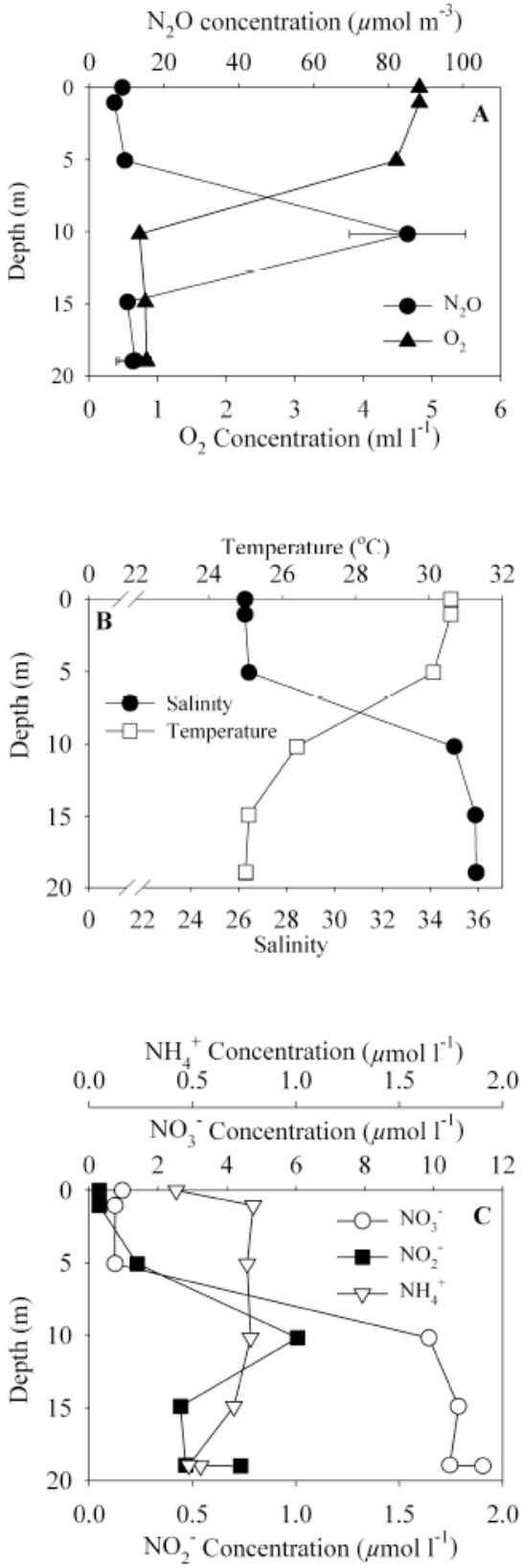

Figure A.18 M12 (July 2008 12:00 PM CST) station 8C depth profiles for (A) N_2O and O_2, (B) temperature and salinity, and (C) NH_4^+, NO_3^- and NO_2^-. Bars represent mean ± S.D.

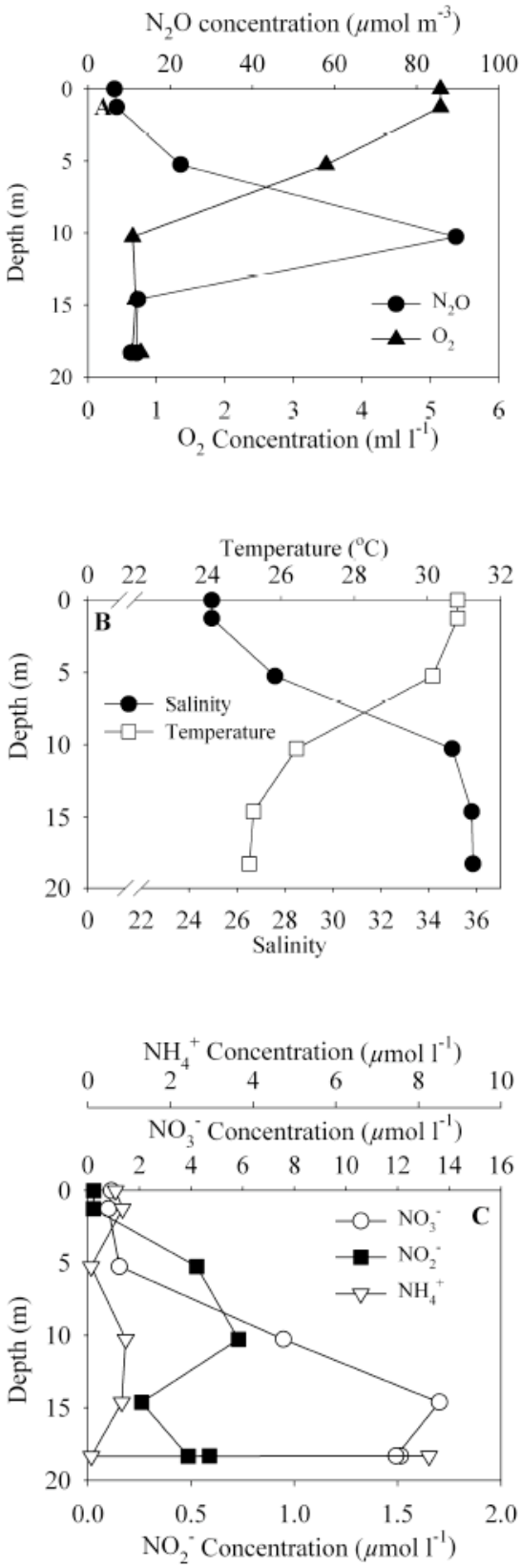

Figure A.19 M12 (July 2008 8:00 PM CST) station 8C depth profiles for (A) N_2O and O_2, (B) temperature and salinity, and (C) NH_4^+, NO_3^- and NO_2^-. Bars represent mean ± S.D.

VITA

Name:	Lindsey A. Visser
Address:	c/o Dept. of Oceanography, Texas A&M University College Station, TX 77843
Email Address:	lvisser@ocean.tamu.edu
Education:	B.S. Marine Biology, Texas A&M University, 2006
	M. S. Oceanography, Texas A&M University, 2009